INVESTIGATION OF THE SUSCEPTANCE PROBE FOR USE IN AN AUTOMATIC WAVEGUIDE MATCHING SYSTEM

A. G. RED

1953

Library
U. S. Naval Postgraduate School
Monterey, California

41-71

INVESTIGATION OF THE SUSCEPTANCE PROBE FOR USE IN AN AUTOMATIC WAVEGUIDE MATCHING SYSTEM

-

A. G. RED

INVESTIGATION OF THE SUSCEPTANCE PROBE FOR USE IN AN AUTOMATIC WAVEGUIDE MATCHING SYSTEM.

by

Arthur George Red
u

Lieutenant, United States Navy.

Submitted in partial fulfillment

of the requirements

for the degree of

MASTER OF SCIENCE
IN
ENGINEERING ELECTRONICS

United States Naval Postgraduate School

Monterey, California

1953

R265

This work is accepted as fulfilling

the thesis requirements for the degree of

MASTER OF SCIENCE
IN
ENGINEERING ELECTRONICS

from the

United States Naval Postgraduate School

The study forming the basis of this report was conducted while the author was attached to the Dalmo Victor Company, San Carlos, California. The assistance rendered and the facilities made available by the personnel of the company, and in particular, by Mr. Glenn A. Walters, Director of RF Research is gratefully acknowledged.

TABLE OF CONTENTS

		Page
List of Illustrations		iv
Table of Symbols and Abbreviations		vi
Summary		vii
Chapter I.	Introduction	1
Chapter II.	Operation of Proposed System	4
Chapter III.	General Discussion of Tuning Probe	12
Chapter IV.	Development of Scanning Principle	17
Chapter V.	Analysis of Scanning Effects	25
Chapter VI.	Utilization of Signal in Servo System	39
Chapter VII.	Experimental Data	51
Chapter VIII.	Conclusion	59
Bibliography		61

LIST OF ILLUSTRATIONS

FIGURE 1 Block diagram of proposed system

FIGURE 2 Transmission line with matching stub

FIGURE 3 Screw admittance on Smith Chart

FIGURE 4 Variation of VSWR with probe depth

FIGURE 5 Variation of $|\rho|$ with probe depth

FIGURE 6 Change in VSWR for various small vertical displacements at various depths

FIGURE 7 Variation of VSWR for given matching probe depth with .025 vertical displacement of sensing probe

FIGURE 8 Microwave circuit

FIGURE 9 Typical plot of Y_{IN} versus probe location for Y probe $= +j0.4$

FIGURE 10 Typical plot of Y_{IN} versus probe location for Y probe $= +j0.6$

FIGURE 11 Four general cases of mismatch

FIGURE 12 Variation of modulation envelope due to components of scanning motion

FIGURE 13 Variation of modulation envelope when matching probe is at position of match

FIGURE 14 Phase sensitive detector circuit

FIGURE 15 (a-d) Error detection operation

FIGURE 16 Partial schematic of servo amplifier

FIGURE 17 Plot of $E_r = R \sin \omega_s t$ as it undergoes phase detection

FIGURE 18 Photograph of equipment used

FIGURE 19 Carriage used for data in Phase I

FIGURE 20 Variation of modulation envelope due to horizontal scanning motion.

FIGURE 21 Variation of modulation envelope due to vertical scanning motion

FIGURE 22 Carriage used for data, Phase II

FIGURE 23 Variation of modulation envelope due to circular scan

FIGURE 24 Proposed mechanical layout of matching device

TABLE OF SYMBOLS AND ABBREVIATIONS

$\mathcal{E}_i$ - Incident electric field

$\mathcal{E}_x$ - Electric field at point x

$\mathcal{E}_r$ - (Where used on diagram) Modulation envelope of reflected wave

R - Amplitude of component of modulation envelope due to horizontal component of scanning motion

P - Power in watts

VSWR - Voltage standing wave ratio

$\bar{Y}$ - Normalized admittance

$\bar{Y}_{IN}$ - Normalized input admittance

$\bar{Y}_{probe}$ - Normalized admittance of probe in waveguide

$\bar{Y}_1$ - Total normalized admittance at point x_1

$\bar{Y}_1'$ - Normalized admittance at probe

$\bar{Y}_1''$ - Normalized admittance of load transformed to x_1

Z_{20} - (As used in data) Position of matching probe on waveguide

β - Constant $2\pi/\lambda$

λ - Wavelength

ρ - Reflection coefficient

ω - Angular frequency of rotation ($2\pi f$)

ω_s - Angular scanning frequency

θ - Departure of resultant phase of modulation envelope of reflected wave from normal 45° degree position

SUMMARY

This paper presents the results of a theoretical and experimental investigation to utilize the susceptance probe in an automatic waveguide tuning system. By means of a servo loop, the probe is positioned longitudinally along the waveguide and at the proper depth to effect a match in the waveguide system. The error signal for servo use is obtained by causing the probe to move in a circular scanning motion. As a result of this scanning motion the reflected wave is modulated, and this modulation envelope serves as the error signal. An error detection circuit is also proposed and discussed.

Experimental confirmation of certain phases of the theory is included.

CHAPTER I INTRODUCTION

Impedance matching is an important design requirement for waveguide feed systems. The recent trend toward broadband operation of radar equipment has greatly increased these requirements, in that low VSWR's across wide bandwidths are required. For any waveguide system at a given frequency, the maximum VSWR may be equal to the product of the VSWR's of the individual components.* The requirement that all components present a minimum VSWR across a band of frequencies presents problems whose solutions are obtainable only after extensive experimental work on the individual components. This is particularly true in the case of inherently narrow band components, such as rotary joints.

The approach used to date to achieve broadband matching in a waveguide system may be described in two phases. First, each component is compensated by adding matching devices at the discontinuities involved. Oftentimes an acceptable match cannot be achieved in this manner due to other considerations. As an example, the combination of a step, a resonant ring, and a capacitive button (as may be used to compensate a rectangular-to-round rotating transition) may result in a power breakdown factor which is too low. Often, therefore, the second phase of the matching procedure is to add a discontinuity at a point remote from the original discontinuities to reduce the standing waves in the system. By experimental means, a matching device is placed in the transmission system at a position which results in the most favorable VSWR across the band of frequencies.

* G. L. Ragan, MICROWAVE TRANSMISSION CIRCUITS, page 609 ff.

Statically positioned matching devices are usually frequency sensitive, and hence a minimum VSWR may be attained at only a few points within a broad band of frequencies. In high power microwave systems, as small a mismatch as possible (as seen by the magnetron) is desirable.* Thus, for an ideal system, the matching device should be moved to present the proper phase of impedance each time that the operating frequency is changed. A broadband matching device has been proposed by Jakes**utilizing a directional coupler. One arm of the coupler is terminated in a short circuited waveguide of variable length. By manually adjusting the length of this arm, the device may be used to match any load over a wide band.

However, if automatic selection of the operating frequency is desired, then a matching device capable of automatically positioning itself to achieve a match in the waveguide system is necessary to satisfy the oscillator requirement.

The automatic system for waveguide tuning to be presented in this thesis utilizes a tuning probe and a servo positioning circuit. Details of the proposed system and a qualitative discussion of system operation will be given in Chapter II to serve as a basis for further analysis. Chapter III will cover the pertinent characteristics of the susceptance probe which illustrate the suitability of the probe for use in an automatic tuning system. Chapter IV deals with the development of the scanning

---

*L.W. Brown, PROBLEMS AND PRACTICE IN THE PRODUCTION OF WAVE GUIDE TRANSMISSION SYSTEMS, page 639 ff.

**W.C. Jakes, BROADBAND MATCHING WITH A DIRECTIONAL COUPLER, page 1216 ff.

principle. Chapter V presents a theoretical analysis of the effects of the probe scanning motion. Chapter VI suggests a servo loop in which the error signal may be used to position the matching probe assembly. In Chapter VII, experimental data supporting certain phases of the theory will be presented.

CHAPTER II OPERATION OF PROPOSED SYSTEM

Figure 1 shows a block diagram of the proposed automatic waveguide matching system. The system consists mainly of a motor driven waveguide tuner, a directional coupler, and a computer amplifier in a servo loop. Changes in the amplitude of the reflected wave, as sampled by the directional coupler, are converted into servo signals to drive the tuning elements to a position of match. The system is to operate across a band of frequencies from 8400 mc. to 9600 mc.

The tuning element consists of a travelling probe driven horizontally and vertically by two-phase motors. Constant sampling of the magnitude of the reflected wave will occur in the detector located in the directional coupler. This signal will be fed into the servo loop, which will act to position the probe so that the proper value of admittance is presented by the tuning probe in the wave guide to achieve a match. In order to achieve directional sense (vertical and horizontal) for servo use, an additional sensing probe, mounted opposite the matching probe and travelling with it, will be caused to scan in a circular path at a constant speed. The plane of this circular path is parallel to the longitudinal axis of the wave guide and perpendicular to the broad faces. This sensing probe motion will cause the reflected wave to be modulated, and this modulation envelope may be extracted and used as a servo signal. The information concerning the position error of the matching assembly with reference to the position of match will be contained in the phase of the modulation envelope. By comparing the modulation envelope with reference phases in a phase sensitive detector circuit, this position information may be derived and applied

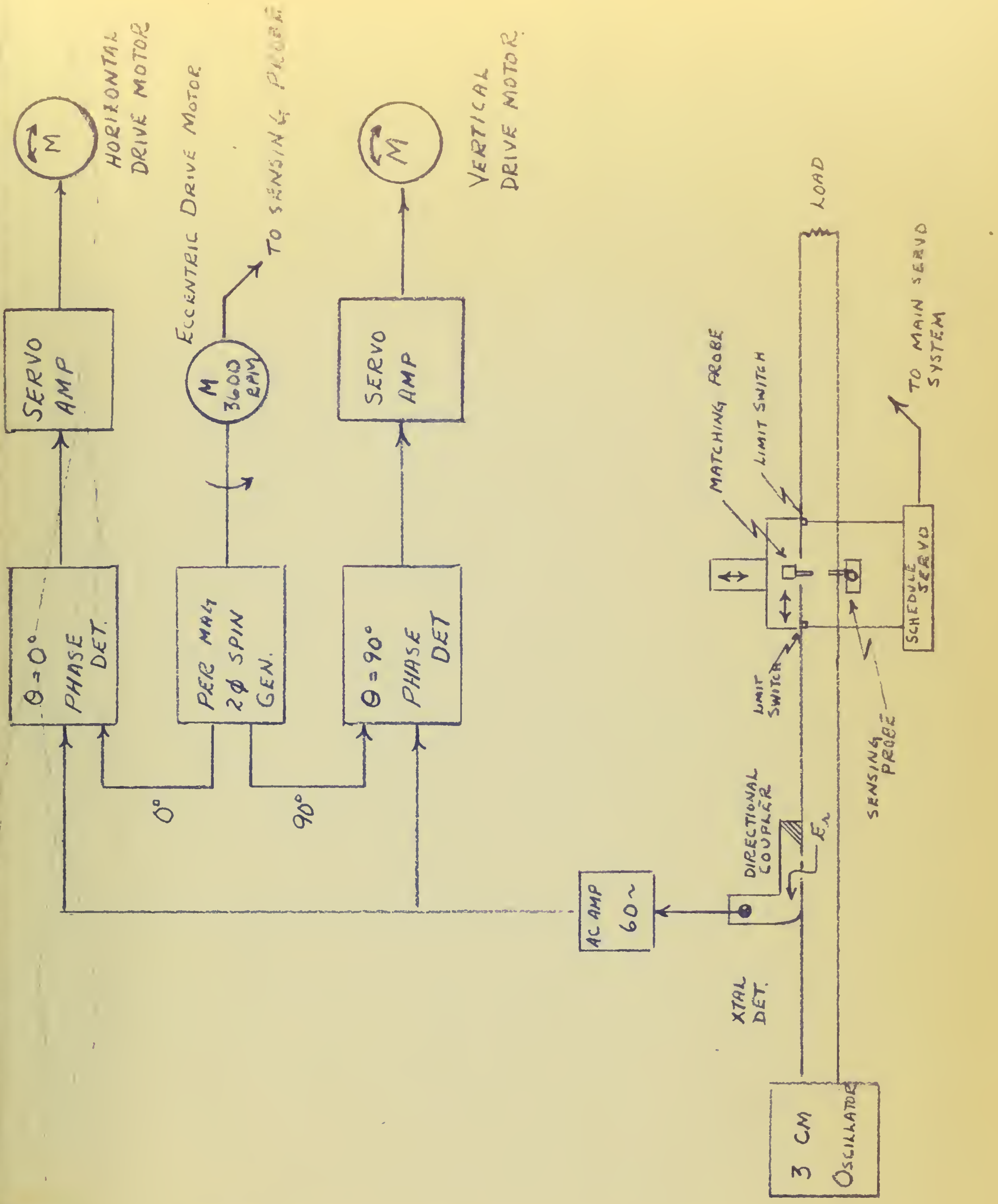
M
HORIZONTAL DRIVE MOTOR
SERVO AMP
θ = 0°
PHASE DET.
0°
ECCENTRIC DRIVE MOTOR
TO SENSING PROBE
M
3600 RPM
PER MAG 2φ SPIN GEN.
90°
M
VERTICAL DRIVE MOTOR
SERVO AMP
θ = 90°
PHASE DET
AC AMP 60~
LOAD
MATCHING PROBE
LIMIT SWITCH
TO MAIN SERVO SYSTEM
SCHEDULE SERVO
LIMIT SWITCH
SENSING PROBE
DIRECTIONAL COUPLER
Er
XTAL DET.
3 CM OSCILLATOR

Fig. 1 Block diagram showing operation of suggested auotmatic system.

to the drive motors.

In addition to the main servo loop a secondary scheduling servo must be included. This servo will be actuated by limit switches placed at each end of the slot in the wave guide. Since proper matching positions occur every half wavelength, measured along the guide, the slot need be only one half guide wavelength at the lowest operating frequency to be used. Hence the scheduling servo will displace the matching assembly one half guide wavelength in the direction opposite to its travel, as it approaches the end of the slot in its search for a position of match.

To illustrate the modulation of the reflected wave by motion of the tuning probe, one may use the more familiar transmission line in an analogy. In this analogy the tuning probe corresponds to a stub tuner as used in matching transmission lines. FIGURE 2(a) shows diagramatically a transmission line with a mismatched load and a stub. Assume that some means is available for sampling the reflected wave amplitude on the transmission line at some point, B, near the generator.

As case 1, assume that the stub located at point A is of the correct length and at the proper position so that the transmission line is matched. Then, no reflected wave amplitude will be measured at B. If the stub is now moved a small distance to the right, a mismatch occurs, and a reflected wave amplitude will appear at B. This amplitude will increase as the stub is moved further to the right. The same holds true if the stub were to be moved in a similar distance to the left of point A. If the stub were mechanically moved with simple harmonic motion

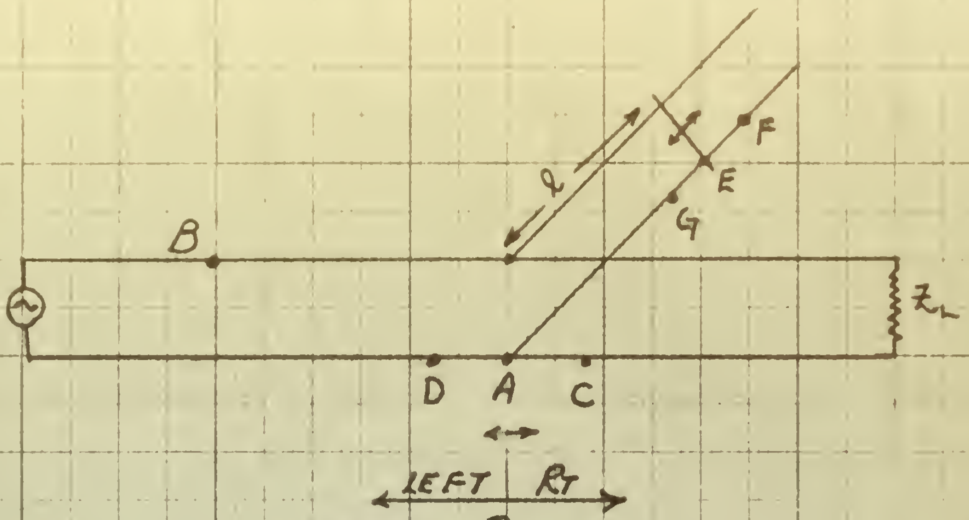
ℓ
F
E
G
B
Z_L
D
A
C
LEFT
RT

FIGURE 2

TRANSMISSION LINE WITH MATCHING STUB

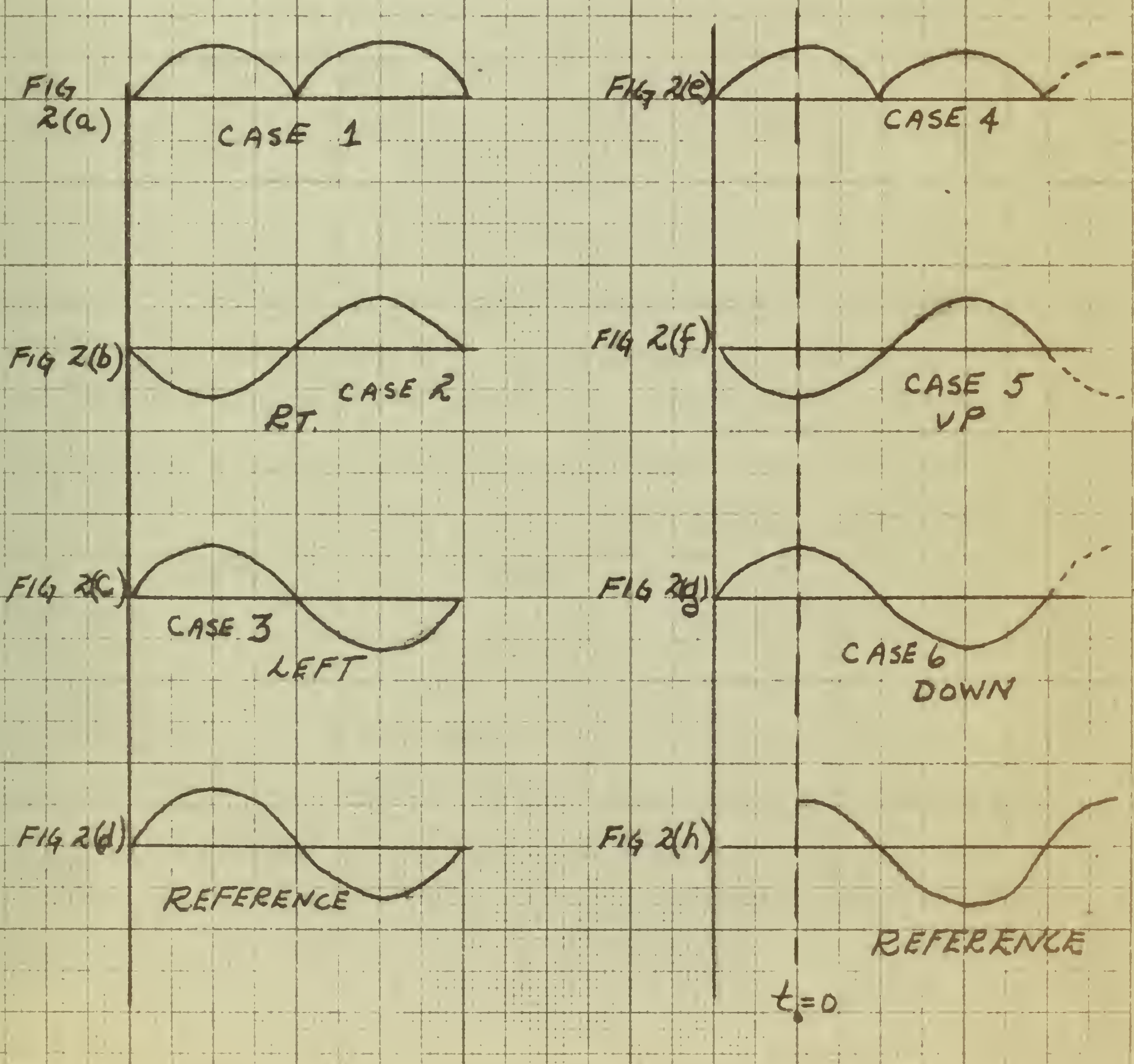
FIG 2(a)
CASE 1
Fig 2(b)
CASE 2
RT.
FIG 2(c)
CASE 3
LEFT
FIG 2(d)
REFERENCE
FIG 2(e)
CASE 4
FIG 2(f)
CASE 5
UP
FIG 2(g)
CASE 6
DOWN
FIG 2(h)
REFERENCE
t=0

through point A for a short distance on either side of point A, then an amplitude variation at point B, similar to that illustrated in FIGURE 2(b) would result. This variation, plotted as a function of time, would be at double the frequency of the mechanical harmonic motion of the stub. This double frequency wave constitutes the modulation envelope signal that results when the stub is moved back and forth through the position of match.

As case 2, consider that the stub is no longer located at the correct match position. Instead, let point C represent the correct position of match. Then an amplitude of reflected wave will be detected at point B. Again move the stub back and forth a short distance on either side of point A, with simple harmonic motion. Assume that the stub moves to the right of point A. As the stub is being moved toward the position of match, the amplitude of the reflected wave will decrease during the stub excursion to the right. On moving the stub to the left of point A, away from the position of match, the amplitude of the reflected wave will increase up to the maximum excursion of the stub, then decrease as the stub returns to point A. FIGURE 2(b) shows the variation in amplitude of the reflected wave just described plotted as a function of time.

For case 3, consider that the correct position for match is at point D. Again move the stub back and forth with simple harmonic motion through point A, with an initial excursion to the right. Following the same reasoning as for case 2, a plot of the variation of the reflected wave amplitude would be shown in FIGURE 2(c).

Note that wave forms 2(b) and 2(c) are 180° out of phase and that the individual phases bear a direct relationship to the position of the stub relative to the desired position of match. FIGURE 2(d) represents a reference voltage related in phase to the mechanical motion of the stub. Waveform 2(b) adds in phase with 2(d); waveform 2(c) adds 180° out of phase. If this addition were to occur in a servo amplifier, the relative phase information could be used to move the stub toward the position of match.

To return to the wave guide system, the left-right motion of the stub corresponds to longitudinal motion of the tuning probe in the waveguide. That this is true is more fully explained in Chapter IV.

The length of the matching stub used on the transmission line is analogous to the depth of penetration of the tuning probe in the waveguide, in that length of the stub may be said to determine the magnitude of the reactive component associated with the stub impedance.* Hence, variations in the length of the stub in our example, correspond to variations in the penetration depth of the probe. Assume that the transmission line in FIGURE 2 requires a short circuited stub of length ℓ, located at point A for a matched line. Let the length of the short circuited stub be variable, to allow for variations in the reactive component of the stub impedance. Again, follow through the actions and reasoning used for the case of horizontal motion described as cases 1, 2, and 3. Only now the stub remains at point A, and the position of

*Note - The relation between probe depth and the magnitude of the susceptance that it presents to the waveguide is discussed at length in CHAPTER III.

the shorting bar along the stub is varied. To follow through:

Case 4 - Shorting bar at E, stub is correct length. Harmonic motion of shorting bar to either side of point E results in modulation envelope as shown in FIGURE 2(e). This is the double frequency variation indicating the match position.

Case 5 - Shorting bar at E, but now F represents correct length for match. Harmonic motion of shorting bar (with initial excursion toward F) results in modulation envelope waveform 2(f).

Case 6 - Shorting bar at E, with G representing correct match length. Harmonic motion of shorting bar (with initial excursion toward F) results in modulation waveform 2(g).

As a final condition, assume that the waveforms 2(e), (f), and (g) are shifted 90° in phase with reference to time $t_o = 0$. This corresponds to making the initial reference time occur when the shorting bar is at its maximum excursion to one side of the reference position. This condition results in a cosine wave with respect to t_o as the form of the modulation envelope. If FIGURE 2(h) represents a reference voltage related in phase to the mechanical motion of the shorting bar, then remarks made concerning phase detection of the modulation envelope for the cases of horizontal stub motion apply here for the cases of changes in length.

Thus it has been shown by a transmission line analogy that scanning motion of the tuning probe longitudinally along the waveguide and also in the vertical (or "penetration") direction results in amplitude

modulation of the reflected wave. Furthermore, phase information contained in the modulation envelope may be used in a servo loop as a position error signal.

CHAPTER III GENERAL DISCUSSION OF TUNING PROBE

The general information presented in this chapter concerns the admittance effect of a probe inserted in a waveguide. It is included as necessary background material for this thesis. It is mostly obtained from Ragan* where further details and corroboration may be found.

A probe introduced into a waveguide parallel to the electric field vector results in a nearly pure susceptance being presented to the waveguide system at that point. This susceptance is capacitive for insertions less than a free space quarter wave length, and inductive for insertions greater than this resonant length. This susceptance behavior is a function of probe diameter. More correctly, it is a function of the ratio of the diameter of the probe to the width of the guide. When this ratio is kept small, the pure susceptance approximation holds more closely and for greater penetration depths.

Since it is usually not practicable to insert a probe of length greater than a quarter wave length into the broad face of a waveguide, only the capacitive susceptance effect will be considered.

To the extent that the pure capacitance approximation holds, the magnitude of the admittance is a direct function of the probe penetration depth. This admittance may be presented in all the possible phases by adjusting the position of the probe longitudinally along the waveguide within a half wavelength as measured along the guide. For small values of insertion, the magnitude and phase of the admittance are independent of each other.

*G. L. Ragan, MICROWAVE TRANSMISSION CIRCUITS

These features establish the versatility of the probe as a matching device. Since the probe may present any admittance in the waveguide, theoretically any VSWR may be set up in a waveguide system. Conversely, by proper adjustment of position and depth, the probe admittance may compensate the mismatch caused by any value of load admittance.

As the depth of penetration of the probe is increased, the voltage breakdown factor of the waveguide is decreased. This determines that a system requiring deep penetration is necessarily limited to low powers. Thus, if used in high power microwave systems, the penetration depth must be kept to a low value or further steps taken to restore the voltage breakdown factor to a safe value.

Specific data concerning X band components is required for use in Chapters IV and V. However, the data is inserted here where it may also serve to illustrate points brought out in this chapter. Figure 3 shows experimental data which demonstrates the capacitive behavior of a 4-40 screw in an X-band waveguide system. Figure 18 illustrates the equipment as set up on a microwave bench except that a short section of .4 x .9 inch ID waveguide, tapped along the centerline of a broad face to hold a 4-40 screw, was used as the termination. A resistive dry load was used to achieve a nearly reflectionless termination at the mouth of the waveguide. By varying the depth of the screw and measuring the resultant VSWR and the distance from the nulls to the plane of the screw, a Smith Chart presentation of the screw admittance was made. This data covered the frequency band from 8500 mc. to 9600 mc.

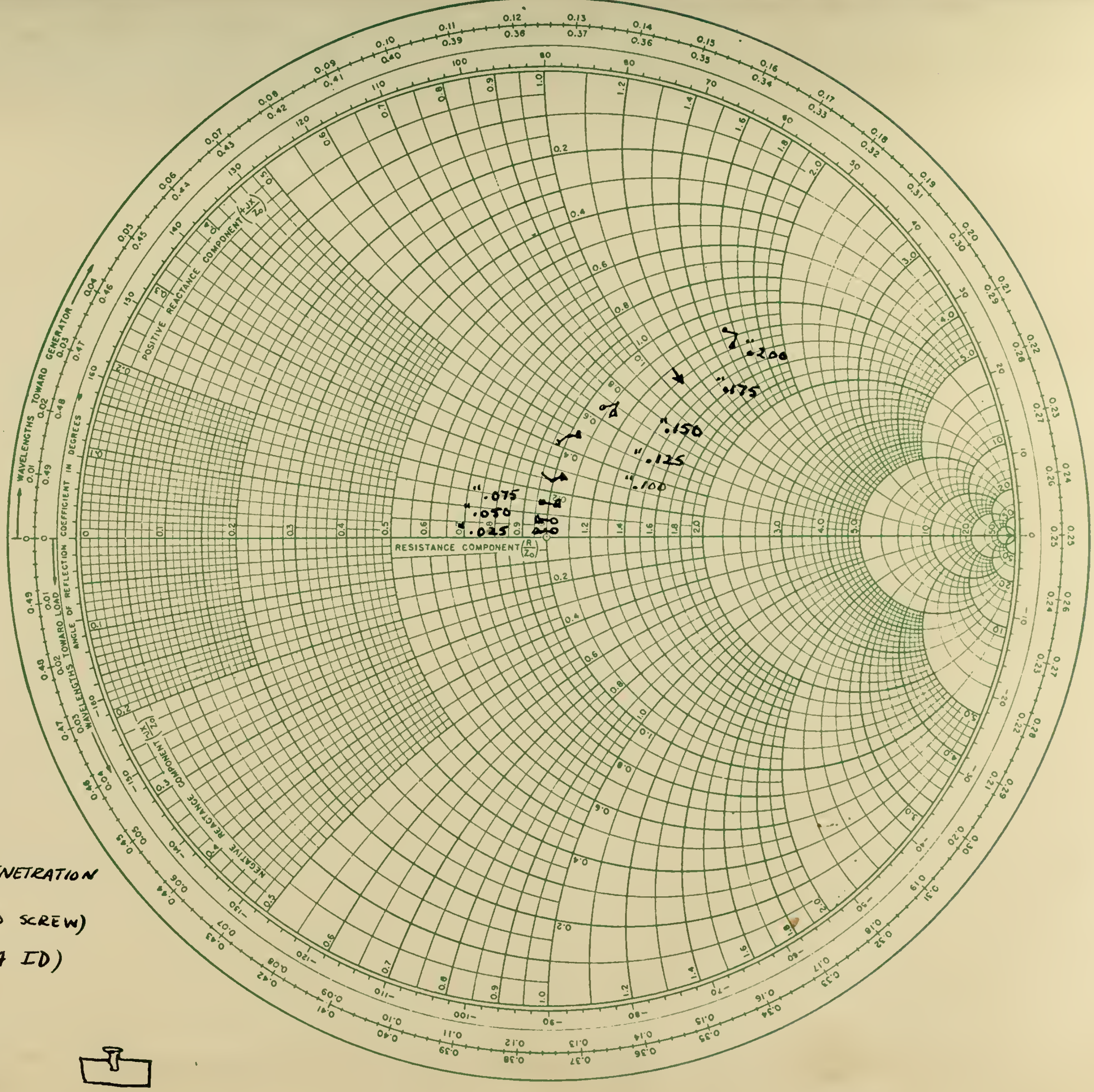

FIGURE 3

PLOT OF ADMITTANCE
AS A FUNCTION OF PENETRATION
DEPTH OF PROBE (4-40 SCREW)
IN WAVEGUIDE (.9 X .4 ID)

9600 MC ·
9000 MC ⊙
8500 MC △

Figure 3 shows that the pure capacitive susceptance approximation holds quite well for penetrations approaching one half guide depth. Frequency independence of the magnitude of the susceptance is also apparent.

The data from Figure 3 was replotted on rectangular coordinates as VSWR versus probe penetration depth for that particular system. This plot constitutes Figure 4 and shows that the penetration depth, if kept within the limits of the range specified above for shunt capacitive susceptance, would limit the VSWR corrections to 4:1. Beyond this penetration depth, the invalidity of the pure C approximation becomes appreciable as does the lowered voltage breakdown factor for the waveguide.

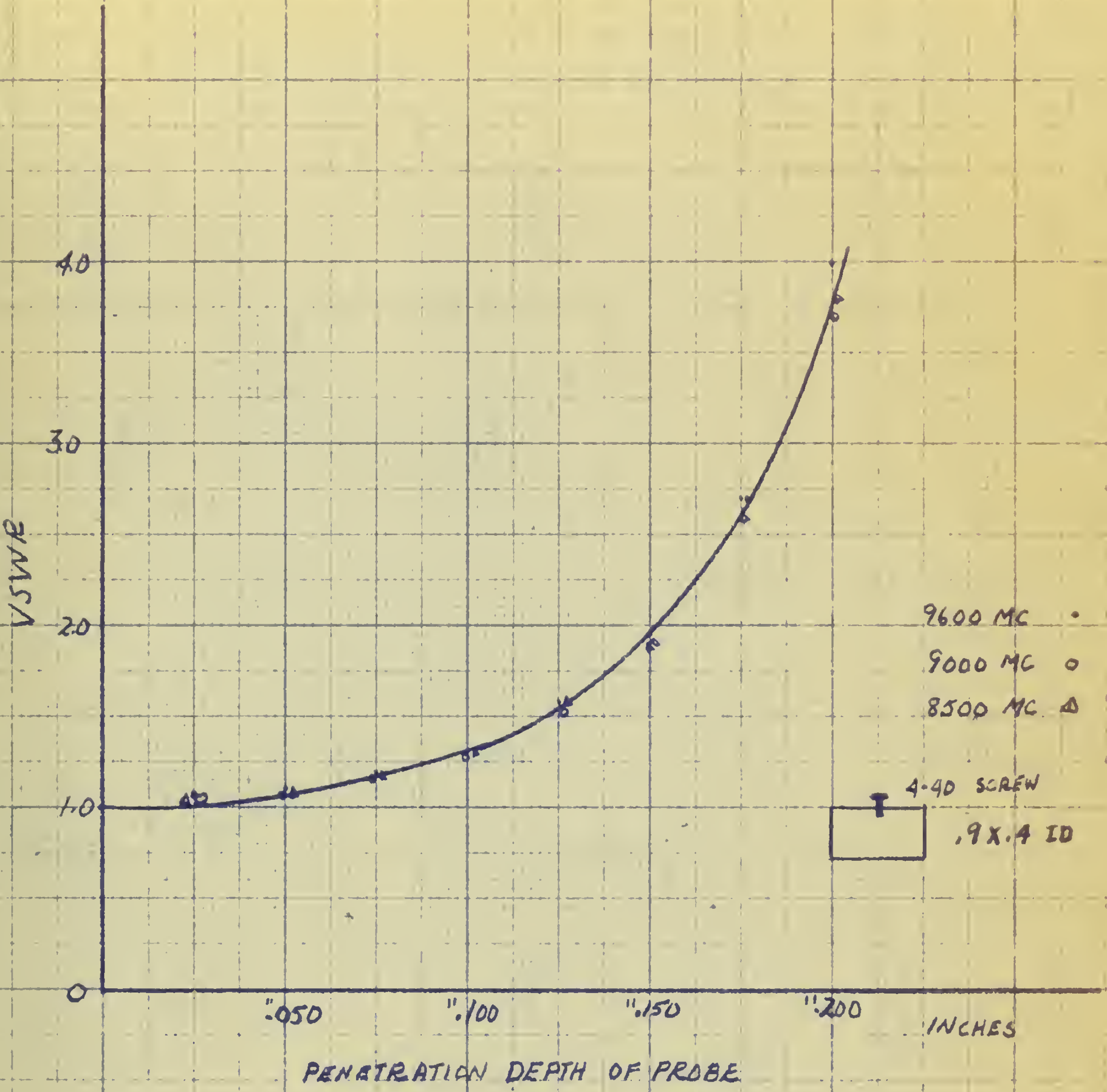
4.0
3.0
2.0
1.0
0
VSWR
".050
".100
".150
".200
INCHES
PENETRATION DEPTH OF PROBE
9600 MC •
9000 MC o
8500 MC Δ
4-40 SCREW
.9 X .4 ID

FIG. 4

CHAPTER IV DEVELOPMENT OF SCANNING PRINCIPLE

FIGURE 4 is a plot of VSWR versus probe penetration depth. This same data may be used to plot the magnitude of the reflection coefficient of the probe, $|\rho|$, versus the probe penetration depth, using the relationship

$$|\rho| = \frac{VSWR-1}{VSWR+1}$$

This curve is shown as FIGURE 5. This curve shows that the magnitude of the reflection coefficient (hence the amplitude of the reflected wave) is a function of probe depth. The function is not linear. However, over small portions of the curve, the variation of $|\rho|$ with small changes in depth can be assumed to be approximately linear. Therefore, the variation in amplitude of the reflected wave for small changes in probe penetration depth may be assumed to be approximately linear. The same approximation may be made in regard to the variation of reflected wave amplitude that would occur for small longitudinal displacements.

Furthermore, if the probe were moved manually in and out for a small distance, about a mean penetration depth, the amplitude of the reflected wave due to the presence of the probe would vary linearly about a mean value. If this variation of penetration depth be made with simply harmonic motion, then the amplitude of the reflected wave would vary sinusoidally with respect to time and in phase with the probe motion. By this same reasoning, harmonic motion of the probe along the longitudinal axis of the guide will result in sinusoidal variation of the amplitude of the reflected wave.* This is an extension of the technique and reasoning used in the transmission line analogy in Chapter II.

---

*Independence of phase and magnitude changes of admittance due to probe are discussed in Chapter III.

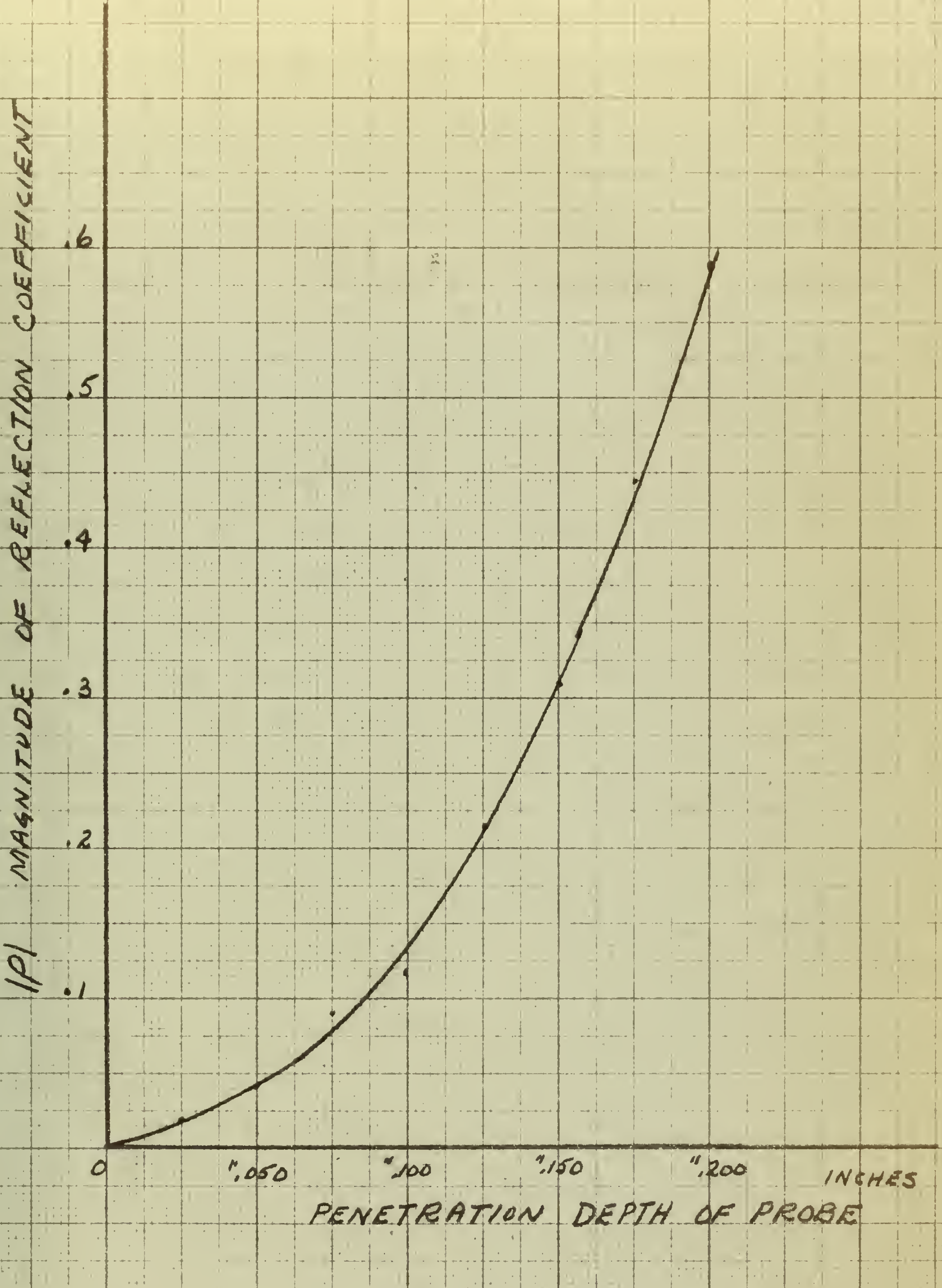

FIG. 5 VARIATION OF $|\rho|$ WITH PROBE DEPTH

[illegible]

[illegible]

[illegible]

achieved. At some time, $t_0=0$, scanning motion of the probe begins. Subsequent horizontal motion toward the position of match will improve the cancellation of the reflected wave, and the amplitude of the reflected wave will decrease. Movement of the probe in the opposite direction will bring about an increase in the reflected wave amplitude. The same reasoning may be applied to vertical motion of the probe. When both motions are combined, the amplitude of the reflected wave will vary as the sum of the separate effects of the scanning motion. But most important is that the phase of each modulation component relative to the phase of the mechanical scanning motion will bear a direct relation to the position of the probe relative to the position of match. This phase information will therefore be contained in the phase of the reflected wave modulation envelope (relative to the mechanical phase of the scanning motion).*

It follows that it may be possible to extract the phase information contained in the modulation of the reflected wave. As this phase information contains direction sense, it might be possible to apply it in some manner to a servo system which will drive the probe to the position of match. The important part of the premise made is that the modulation of the reflected wave contains a "sine" component and a "cosine" component, due respectively to the separate components of mechanical motion of the probe in its circular motion.

A flaw appears in the plan to scan the matching probe. The variation of the amplitude of the reflected wave for small vertical displacements of the probe is not constant for all penetration depths.

---

*The action discussed in this paragraph is given a very limited treatment here since it is more fully covered in the treatment of scanning effects given in the next chapter.

For relatively deep penetrations, a small variation in depth produces a much greater variation in VSWR than occurs at lesser penetrations with the same depth variations. FIGURE 6 is a plot of the derivative (with respect to Δ depth) of the curve in Figure 4, and shows the variation in VSWR for several values of vertical displacements at the penetration depths under consideration. Further investigation showed that the scanning motion could be divorced from the matching probe by placing an additional probe in the broad face of the guide just opposite the main probe. Then the effect of making small changes in the penetration depth of this second probe on the VSWR is the same for all values of penetration of the matching probe. The waveguide section used previously to obtain the data for FIGURE 3 was altered by the addition of another 4-40 screw in the broad face opposite to the first screw. Data was then taken using the same bench setup described in Chapter III. This data appears in FIGURE 7 to support the statement concerning the effect of the second probe. The approximation of the linear behavior of the VSWR for small vertical displacements of the probe at all penetration depths is considered to be achieved.

Hence the scanning motion will be assigned to a second probe, hereinafter called the "sensing" probe. The broad band feature desired in this device requires that the sensing probe be mounted vertically opposite the matching probe. The electrical position of the sensing probe in the waveguide system must always be the same as that of the matching probe. At a given frequency this would allow a half guide wave length displacement in either direction, but a change in operating frequency changes the wave length in the waveguide. Thus, the sensing

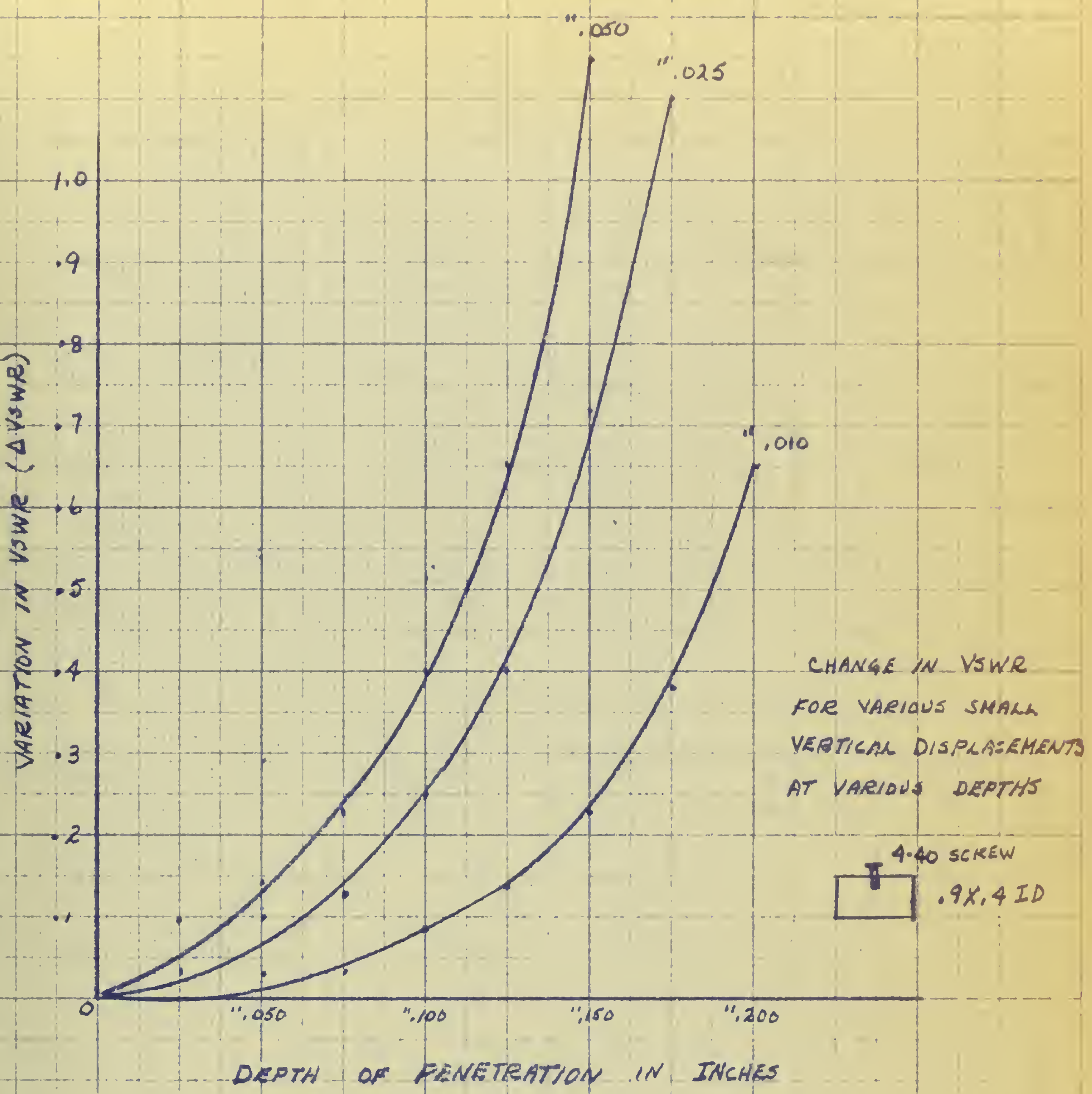".050
".025
".010
1.0
.9
.8
.7
.6
.5
.4
.3
.2
.1
0
".050
".100
".150
".200
VARIATION IN VSWR (ΔVSWR)
DEPTH OF PENETRATION IN INCHES
CHANGE IN VSWR
FOR VARIOUS SMALL
VERTICAL DISPLACEMENTS
AT VARIOUS DEPTHS
4-40 SCREW
.9X.4 ID

FIG. 6

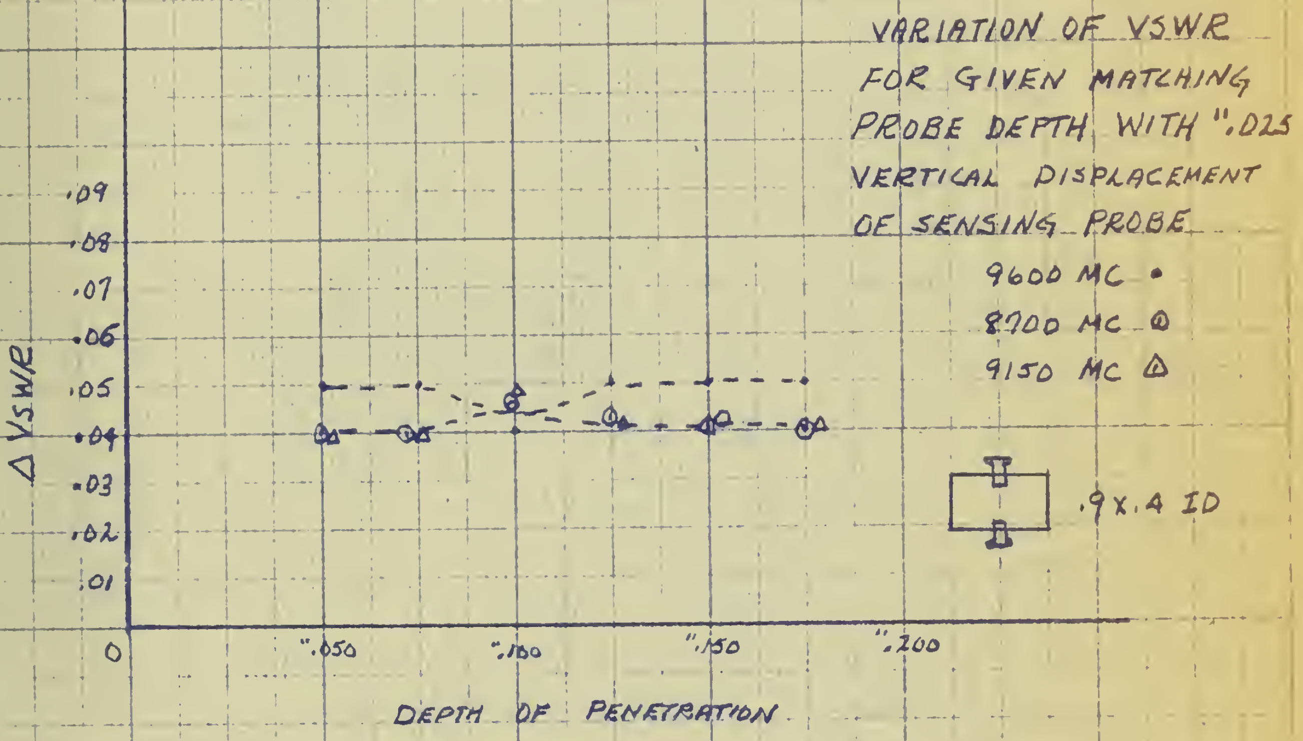

VARIATION OF VSWR FOR GIVEN MATCHING PROBE DEPTH WITH ".025 VERTICAL DISPLACEMENT OF SENSING PROBE

FIG. 7

probe must either change its position relative to the matching probe for each frequency change, or take the position just opposite the matching probe in the waveguide and travel with the matching probe along the waveguide.

CHAPTER V ANALYSIS OF SCANNING EFFECTS

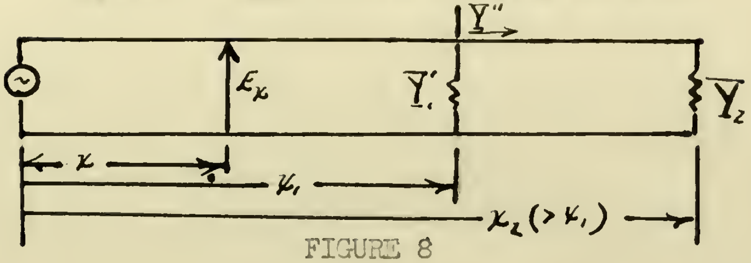

FIGURE 8

A waveguide system containing a susceptance probe at some position x_1 is shown in FIGURE 8. Let the point at which it is desired to examine the electric field be at distance x, measured from the generator. Then

$$\mathcal{E}_x = \mathcal{E}_i e^{-j\beta x} + \rho_1 \mathcal{E}_i e^{-j\beta(2x_1 - x)}$$

where

E_x = resultant electric field at point x $(x < x_1)$

E_i = incident electric wave at sending end

ρ_1 = reflection coefficient at x_1. x, x_1, and x_2 are distances measured along the waveguide as shown.

The effect of scanning the probe in the circular path described in Chapter IV is to cause ρ_1 and x_1 to vary as some function of the scanning frequency. This in turn causes the admittance at x_1 to vary. It must be noted however that the admittance at x_1 consists of the admittance of the probe in parallel with the load admittance transformed to x_1.

Hence, let

Y_1 = total normalized admittance at x_1

Y_1' = normalized admittance of the probe

Y_1'' = normalized admittance of load transformed to x_1

ρ_1 = reflection coefficient at x_1

ρ_2 = reflection coefficient at x_2

Then

$$\bar{Y}_1 = \bar{Y}_1' + \bar{Y}_1''$$

$$\bar{Y}_1'' = \frac{1 - \rho_2 e^{-j\beta(x_2 - x_1)}}{1 + \rho_2 e^{-j\beta(x_2 - x_1)}}$$

$$\rho_2 = \frac{1-\bar{Y}_2}{1+\bar{Y}_2} \qquad \rho_1 = \frac{1-\bar{Y}_1}{1+\bar{Y}_1} = \frac{1-(\bar{Y}_1'+\bar{Y}_1'')}{1+(\bar{Y}_1'+\bar{Y}_1'')}$$

Longitudinal displacement of the probe along the waveguide changes $\bar{Y}_1''$. Vertical displacement of the probe changes $\bar{Y}_1'$. Hence investigation of the effects of some form of perturbation in $\bar{Y}_1''$ and $\bar{Y}_1'$ would involve such mathematical complexities that a more direct method of approach seems desirable.

Since the problem may be studied from the point of view of the admittance of the waveguide at x (looking toward the load) the Smith Chart may be used to illustrate the matching operation for a given set of conditions. For illustrative purposes let

$$\bar{Y}_{LOAD} = 3.0$$

$$(x_2 - x) = \tfrac{3}{4}\lambda$$

As impedances are repeated every half wave length, measured along the waveguide, the effect of the matching probe admittance need only be investigated at a number of points within one half wave length from the load. FIGURES 9 and 10 show the locus of $\bar{Y}_{IN}$ for values of $\bar{Y}_{probe} = +j0.4$ and $\bar{Y}_{probe} = +j0.6$ respectively, for eight positions of the stub along the waveguide. It may be seen that the locus of $\bar{Y}_{IN}$ forms a closed loop, more or less elliptical in shape, as the position of the probe is varied over a half wave length, measured along the waveguide. Comparison

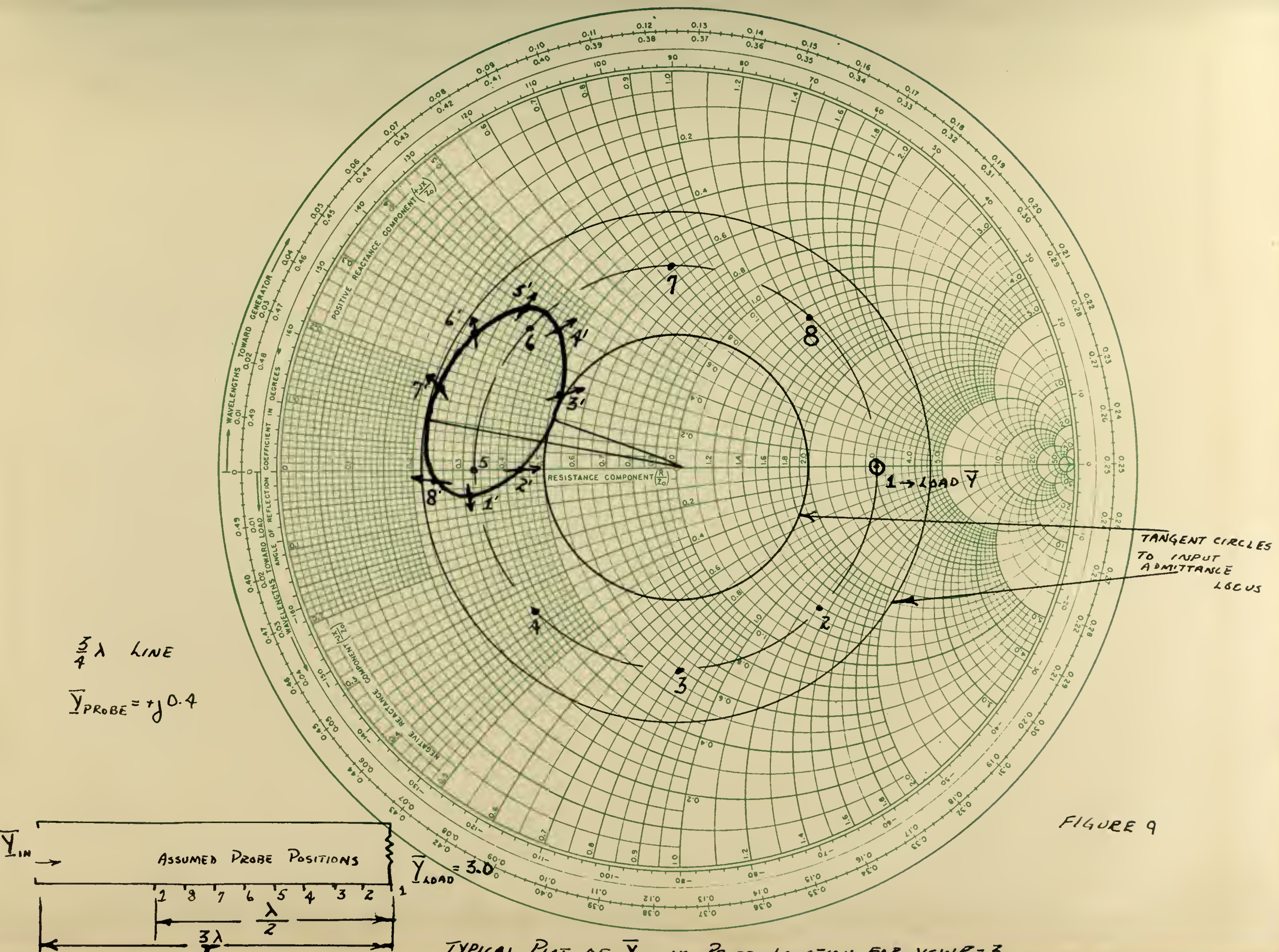

$\frac{3}{4}\lambda$ LINE

$\overline{Y}_{PROBE} = +j0.4$

FIGURE 9

TYPICAL PLOT OF $\overline{Y}_{IN}$ VS PROBE LOCATION FOR VSWR=3

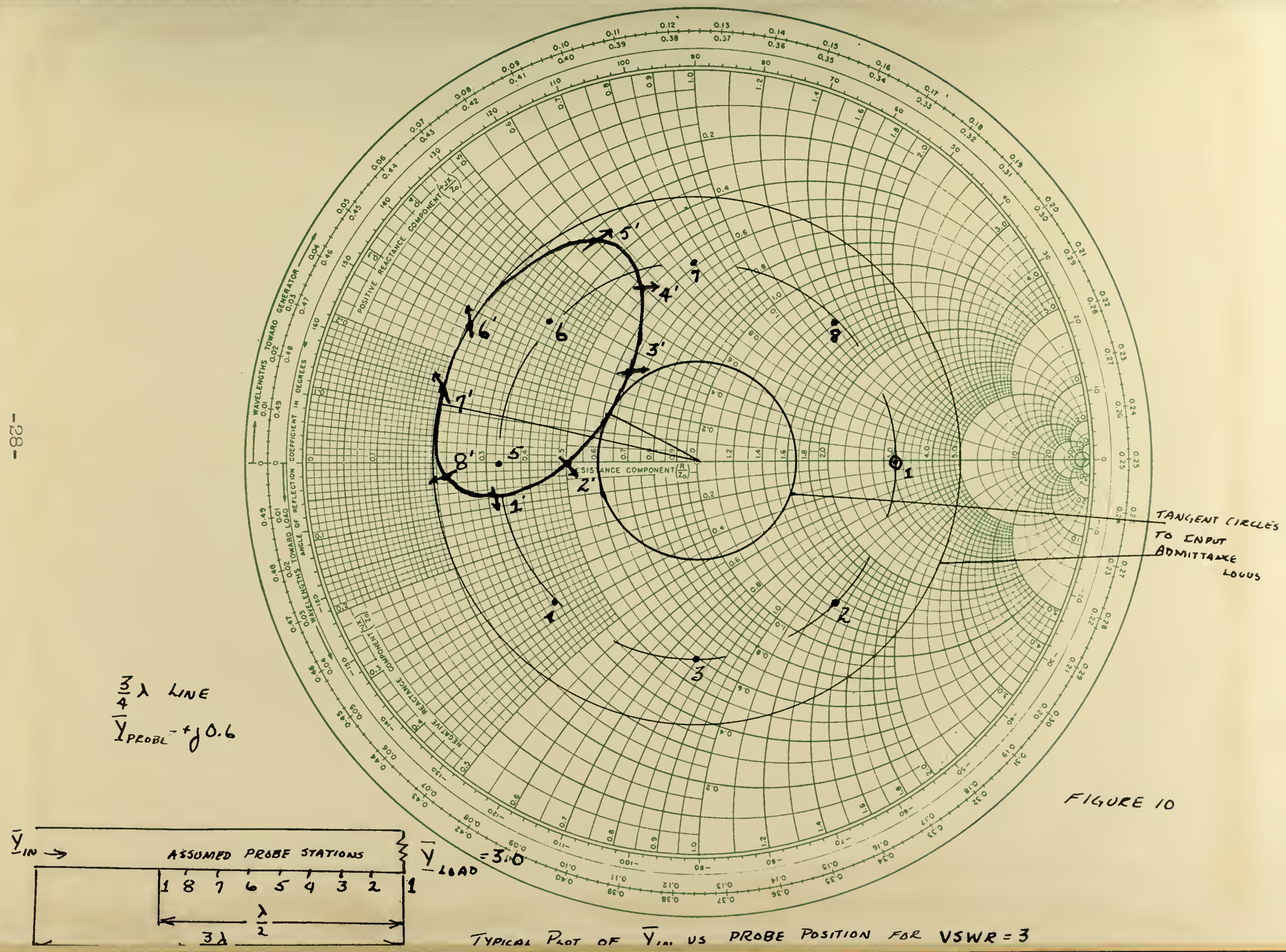

$\frac{3}{4}\lambda$ LINE

$\overline{Y}_{PROBE} = +j0.6$

FIGURE 10

TYPICAL PLOT OF $\overline{Y}_{IN}$ VS PROBE POSITION FOR VSWR = 3

of the two figures shows that as $\overline{Y}_{probe}$ increases the "elliptical" locus gets larger.

By drawing the inner tangent circle to the input admittance locus the probe location that gives the lowest VSWR for the value of $\overline{Y}_{probe}$ used may be found. In both cases, this longitudinal position is seen to be between stations 2 and 3. The longitudinal position that gives the highest VSWR may be determined by drawing the outer tangent circle to the input admittance locus. This position for both cases lies between stations 7 and 8.

Investigation of the effects of the scanning motion of the probe may be carried out using FIGURE 9. Considering first the longitudinal motion of the probe, the admittance plot shows that movement of the probe from one station to another causes $\overline{Y}_{IN}$ to move along the elliptical locus. As the VSWR changes with changes in $\overline{Y}_{IN}$, it follows that the amplitude of the reflected wave must vary also. Let the nominal position of the matching probe be at station 2. Small excursions to either side of station 2, corresponding to the horizontal component of scanning motion, will result in variations in $\overline{Y}_{IN}$, hence in the amplitude of the reflected wave. A similar variation in reflected wave amplitude occurs if matching probe is at station 4, undergoing slight displacements to either side of station 4. A very important difference in the variations does exist however. If the initial excursion of the sensing probe is always in the same direction - say toward station 1, for any position of the matching probe assembly - then the phase of the resultant variation in reflected wave amplitude due to horizontal

scanning motion experienced at station 2 is opposite to that experienced at station 4. To state more simply, with the probe at station 2, a longitudinal excursion toward station 1 increases the reflected wave amplitude. With the probe at station 4, a similar excursion toward station 1 decreases the reflected wave amplitude. The position of most favorable match lies at the point of tangency between stations 2 and 3. Hence, the phase of the modulation envelope of the reflected wave relative to the phase of the mechanical horizontal scanning motion depends upon the position of the probe relative to the position of match. This substantiates the observation made in Chapter II using the transmission line analogy.

An increase in probe length results in an increase in probe susceptance.* The effect of an increase in probe susceptance at each station is shown by the small arrow at that station. In order to visualize the effects of the vertical scanning motion, (which effectively varies the susceptance) it is necessary to recall that for the particular cases shown in FIGURES 9 and 10, the probe susceptance is inadequate to achieve a match. Thus, in FIGURE 9, the arrows in the region of the position of most favorable match show that for vertical excursions toward greater probe depth, the value of the reflected wave amplitude decreases. For excursion in the opposite direction, the reflected wave amplitude increases. If one visualizes the locus of $\overline{\underline{Y}}_{w}$ that would result for a much greater value of $\overline{\underline{Y}}$ probe, (so that the admittance point 1 + j0 is enclosed in the locus), the opposite sensing would be obtained.

---

* Discussed in Chapter III.

In this case the amplitude of the reflected wave would increase for a probe excursion toward greater depth. Hence the phase relationship between the modulation envelope resulting from the vertical scanning motion and the mechanical scanning motion does exist.

A vertical sensing ambiguity is apparent however. If the matching probe is at stations 6, 7, 8, (in FIGURE 9), the arrows show that a decrease in probe susceptance is erroneously indicated. Longitudinal travel of the matching probe assembly toward the position of match would soon correct this ambiguity. But for the time that this ambiguity exists, some provision in the vertical positioning mechanism must be made to prevent the probe from withdrawing completely from the waveguide. Or, considering the opposite case where the vertical sensing may call erroneously for greater penetration, some provision must be made to prevent the probe from striking the opposite face of the waveguide. These provisions may be in the form of a positive stop and a magnetic clutch arrangement in the vertical drive system.

Next, consider the scanning effects when the probe is at a position of match. By following the reasoning used previously in connection with FIGURE 9, scanning motion in each direction will produce the double frequency modulation envelope variation indicated as the match position signal in Chapter II. Again, this requires that one consider the locus passing through the normalized admittance point $1 + j0$, to observe the double frequency effect in connection with the vertical component of the scanning motion.

There is another possible position of the matching probe where scanning will produce a double frequency effect. This is the position where

the outer circle is tangent to the locus, the "least favorable" position. On FIGURE 9 this occurs between stations 7 and 8. At this point the horizontal component of scanning motion will produce a double frequency wave. This is a position of instability however, for on either side of this position the normal error signal will be generated. Furthermore, once the matching probe moves off this position there is no tendency for it to return. This is not the case at the correct position of match. In the particular case in FIGURE 9, should the probe move through station 8 from this unstable position the schedule servo will cause the matching assembly to move back to the region of station 1, whence the normal searching procedure will continue.

As a final note, it is apparent that the amplitudes of the separate components of the modulation envelope will not be constant as the matching probe passes through all the stations. Neither one will go to zero however, nor will both component amplitudes be a minimum at the same time.

As described in Chapter IV, the sensing probe will move in a circular path, the plane of this path being parallel to the long dimension of the waveguide system. If the depth of penetration of the sensing probe varies as the cosine of the angle of rotation of the probe, the horizontal displacement of the sensing probe will vary as the sine of this angle of rotation. The effect of these components of motion of the probe on the reflected wave amplitude will also bear a cosine-sine relationship to each other. Therefore, the modulation envelope of the reflected wave will represent the sum of these two components. This

modulation envelope is the AC signal available to the servo system as an error signal.

For the addition of a sine wave and a cosine wave of equal angular frequency the following general rules hold:

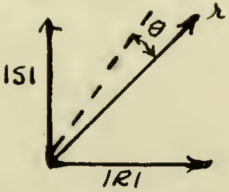

(a) If the amplitudes are equal the resultant will be a sine wave of 1.41 times the amplitude of either component and advanced 45° in phase with respect to the original sine component.

(b) If the amplitudes are unequal the resultant will always be greater than either component and the phase advance will be $45^\circ + \theta$ with θ representing the angle

$$\theta = \tan^{-1} \frac{|S|}{|R|} - \frac{\pi}{4}$$

θ may be negative.

Since the amplitude of the separate components of the modulation envelope will in general not be equal, condition (b) above will usually prevail. The effect of this inequality of amplitudes will be discussed further in Chapter VI under phase detection.

To observe how the direction sense contained in the separate components of the modulation appears in the modulation envelope waveform, refer to FIGURES 11 and 12. FIGURE 11 shows the four general cases of mismatch. FIGURE 12 shows the modulation components as they are generated, and the resultant modulation envelope as it will appear as a result of the addition of the pairs of components. Note that the scanning circle is traversed by the sensing probe always in the same direction.

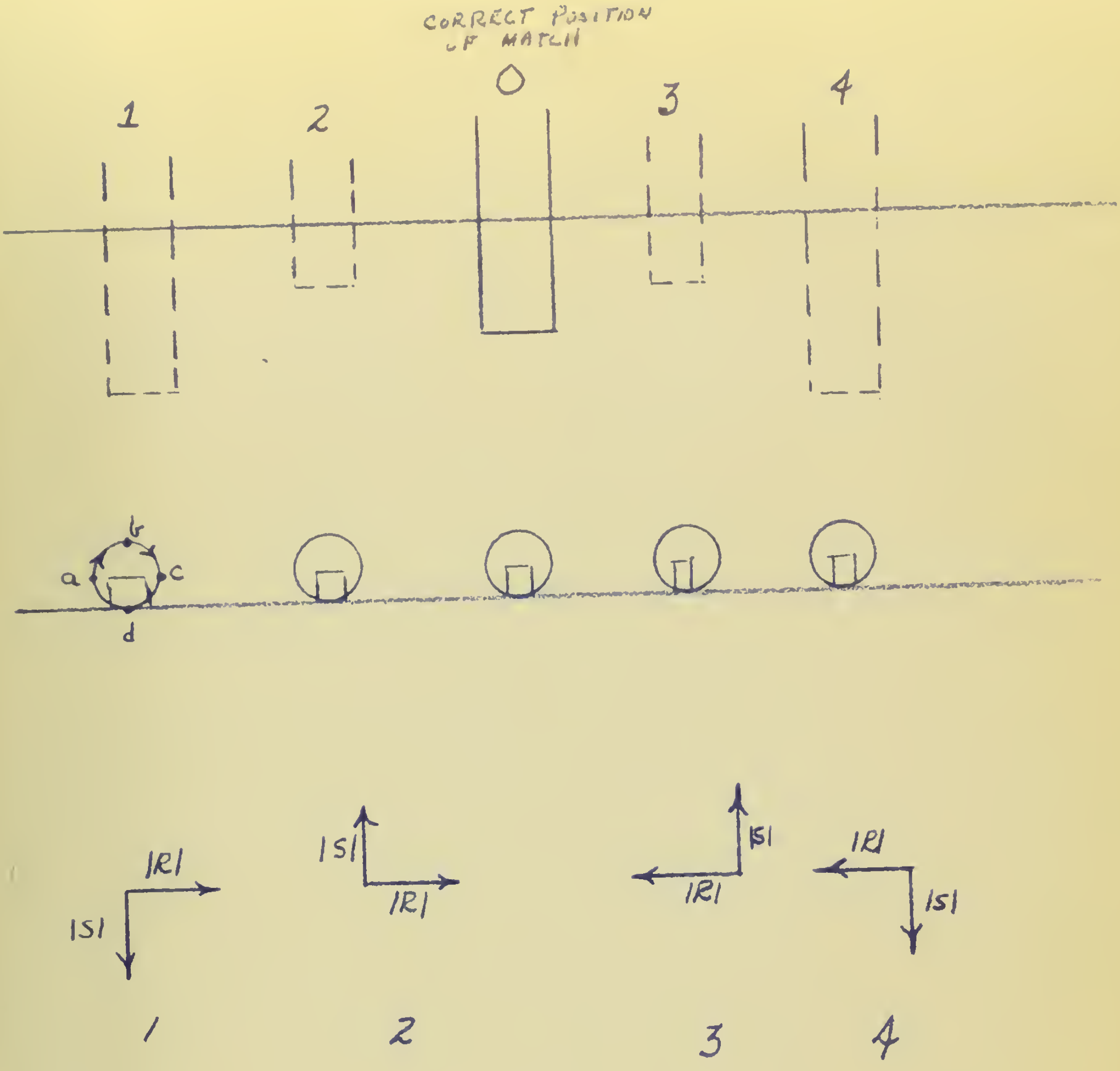
CORRECT POSITION
OF MATCH
1
2
0
3
4
a
b
c
d
|R|
|S|
|S|
|R|
|S|
|R|
|R|
|S|
1
2
3
4

FIG. 11 The four general cases of positions of mismatch of probe in waveguide , shown relative to the position of match.

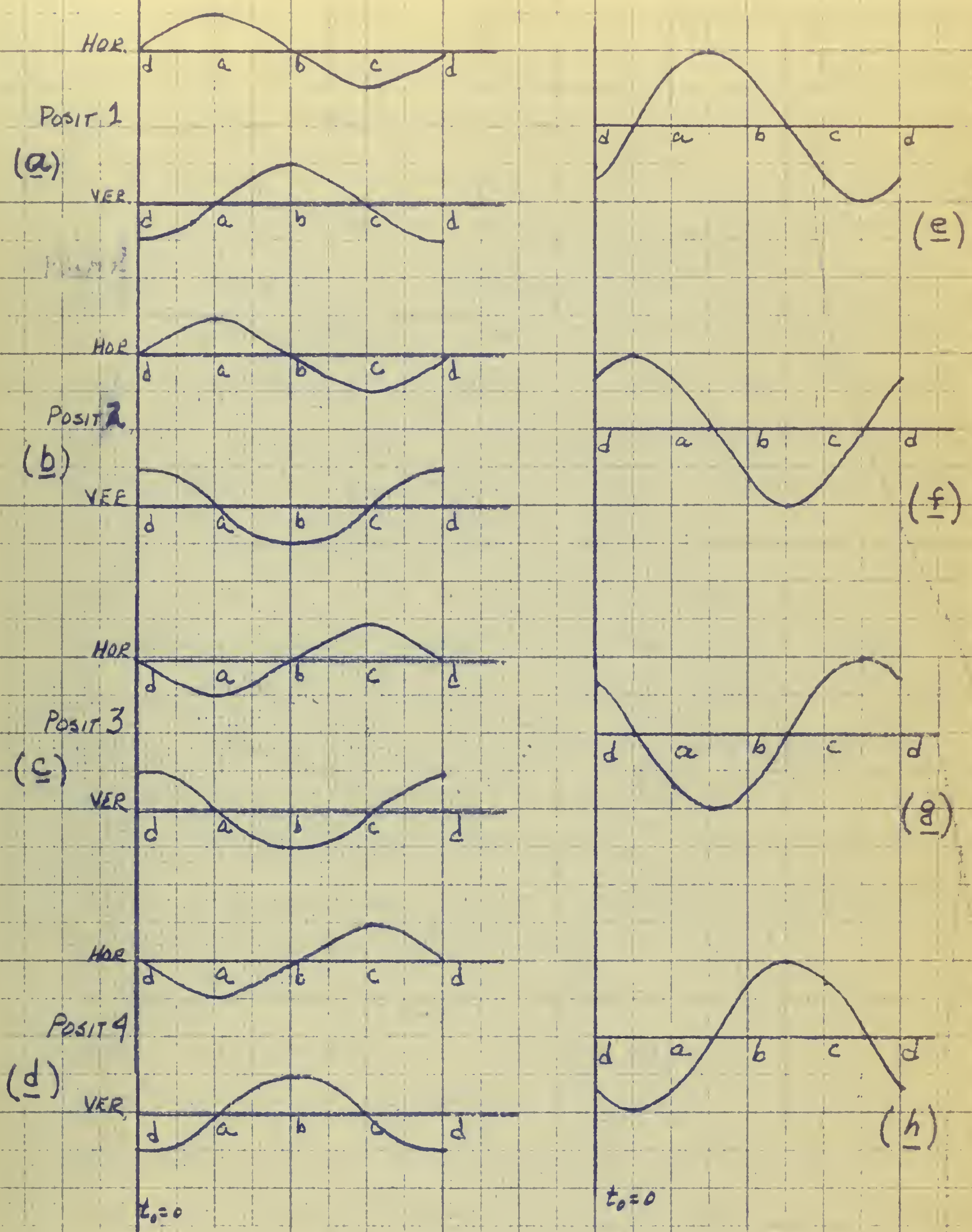

FIG. 12 Variation of E_r due to components of scanning motion of sensing probe for various positions of mismatch

The positions of the matching assembly shown in FIGURE 12 correspond to those indicated in FIGURE 11, as do the lettered points on the scanning cycle. Consider qualitatively the resulting variation of the amplitude of the reflected wave when the matching assembly is at the point of mismatch (position 1, FIGURE 11). As the sensing probe moves from "d" to "a", the component of the reflected wave modulation due to horizontal motion increases, since probe is moving further away from the correct horizontal position of match, reaching a maximum at "a". At the same time the vertical component of the reflected wave modulation decreases, reaching zero at "a" since the depth represented by "a" is the reference depth for the sensing probe. From "a" to "b", the horizontal component decreases, reaching zero at "b", which is the reference horizontal position. The vertical component continues to increase, since the effect of added probe depth is to increase the mismatch. From "b" to "c", the horizontal component continues to decrease, reaching a minimum at "c". The vertical component decreases also, since the effective probe depth is decreasing, which is as desired. From "c" to "d", the horizontal component begins a return to zero, the vertical component continues to decrease toward the minimum.

Hence, the effect of the scanning probe is to add two components to the reflected wave E_r, one a varying as the sine of the scanning angle, the other as the cosine of the scanning angle. Application of the same reasoning at positions 2, 3, and 4, will result in the component variations as shown in FIGURES 2(b), 2(c), and 2(d). It is seen that the phases of the components relative to each other at the time in the initiation of the scanning cycle, $t_o = o$ are set mechanically by the

initial position of the matching assembly along the guide relative to the ultimate position of match. It will be assumed that the assembly is always in the waveguide system and at a random position when the system is energized.

The resultants due to the addition of the horizontal and vertical components are shown in FIGURES 2(e)-(h), plotted against the zero time reference $t_o = 0$, used for FIGURE 2(a)-(d). These are seen to be sine waves of varying phases corresponding to the relative phases of their sine and cosine components as modified by the addition process, noted previously.

Next, it is important to consider the form of the reflected wave modulation when the matching probe is at a position of match, and the sensing probe is scanning. This is best done by the technique just used. Referring to FIGURE 11, the matching probe is considered to be at position "O". In a manner similar to that used in FIGURE 12, the waveforms of the components of the modulation envelope due to scanning are shown in FIGURE 13. At a position of match, all the reference points, a, b, c, d, on the scanning cycle used as in FIGURE 11, represent position of maximum reflected wave amplitude due to scanning motion. Thus, the horizontal and vertical components vary at twice the scanning frequency and the resultant also varies at twice the scanning frequency.

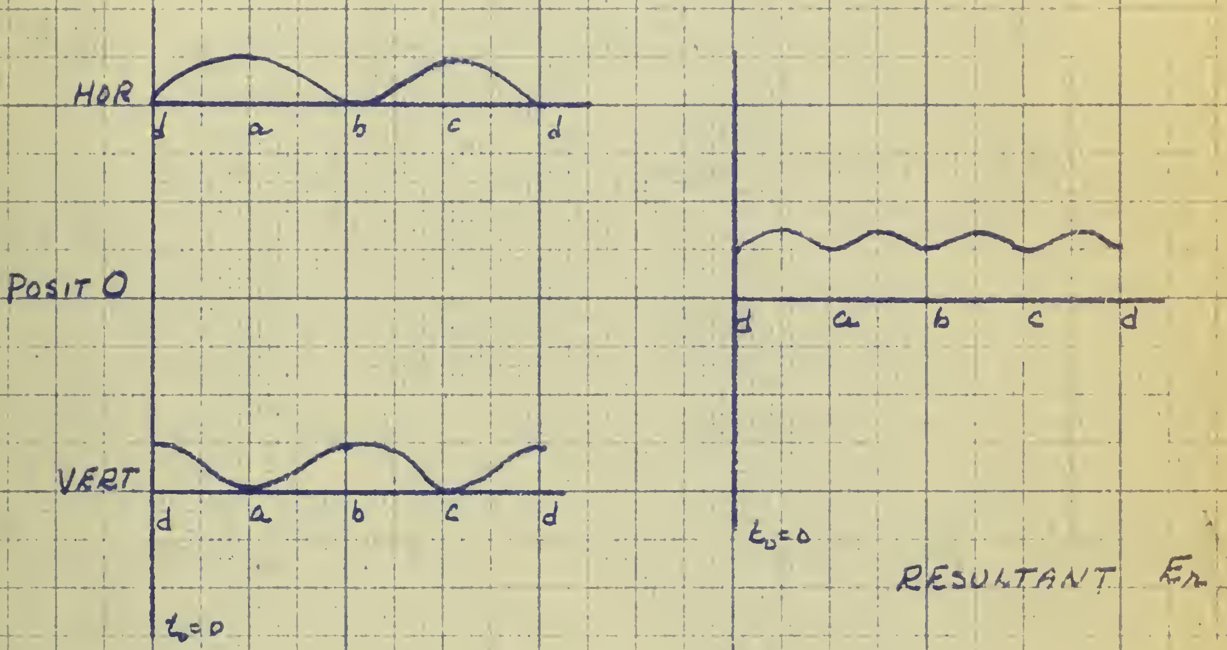
HOR
d
a
b
c
d
POSIT O
VERT
d
a
b
c
d
$t_0=0$
d
a
b
c
d
$t_0=0$
RESULTANT E_r

FIG. 13 Waveforms of components of E_r due to scanning motion when matching probe is at a position of match.

CHAPTER VI UTILIZATION OF SIGNAL IN SERVO SYSTEM

It has been shown that the effect of the circular scanning motion on the reflected wave is a sinusoidal variation in amplitude. The phase of this wave is related to the phase of the components of the mechanical scan as a function of the direction of the error of position of the matching assembly with respect to the position of match. As the modulation envelope of the reflected wave is of interest, it may be extracted and amplified in an audio frequency amplifier to any desired level.

The directional sense for servo use is carried in the phase of the modulation envelope with respect to the corresponding mechanical phases of the components of motion of the circular scan. These reference phases may be presented electrically by the output of a two phase generator geared mechanically to the sensing probe. The mechanical scan components then appear as an electrical sine and a cosine wave representing the horizontal and vertical components respectively. By comparing the phase of the modulation envelope with the reference phases, the required servo directional sense may be extracted.

One such phase comparison circuit is the phase sensitive detector shown in FIGURE 14. Here the reference phases are each added to, and subtracted from the modulation envelope and the resultants are detected so that two pairs of DC levels result. These DC levels represent the degree to which the modulation envelope was in phase with each reference phase and its 180° image. The servo direction sense carried by the phase of modulation envelope now appears as the difference between the DC levels in each pair.

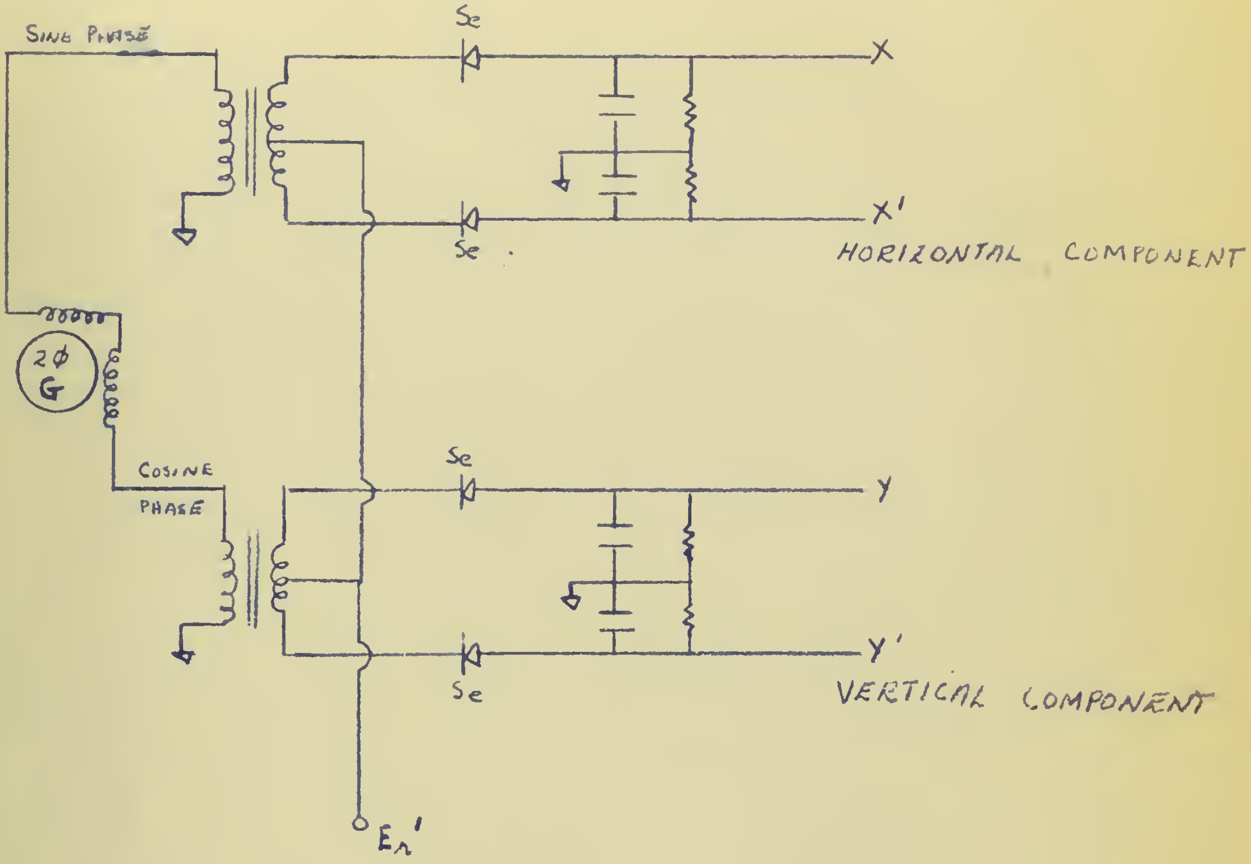
SINE PHASE
Se
X
X'
Se
HORIZONTAL COMPONENT
2φ
G
COSINE PHASE
Se
Y
Y'
Se
VERTICAL COMPONENT
E_r'

FIG. 14 Phase sensitive detector circuit.

This action can be illustrated for the general cases shown in FIGURE 11, where the resultant modulation envelopes for each of the four possible cases of mismatch are as shown in FIGURE 12 (e-h). FIGURE 15 (a-d) shows the reference sine and cosine phases as they appear on each side of the secondaries of the transformers in the phase sensitive detector. Each of these is assigned a direction to correspond to the desired direction of servo motion, (as illustrated in FIGURE 11), for the various positions. The modulation envelopes of FIGURE 2 (e-h) are plotted on these reference phases, maintaining the same relative phase as was used in FIGURE 12 (i.e., $t=t_o = 0$). The resulting waves, as seen by the diode detectors, are shown. The magnitude of the DC levels that result may be deduced from the relative magnitudes of the waves so that if servo motion were made to occur in the direction indicated by the dominant DC levels in each case, the proper correction of the position of the matching probe assembly would be made.

FIGURE 15(a) shows that the dominant DC levels, hence the position corrections, are "right" and "up", which corrections are seen to be required from FIGURE 11. Similar comparisons may be made between positions 2, 3, and 4, from FIGURE 11 and FIGURES 15 (b), (c) and (d), respectively.

A partial schematic for an error detector and servo system is shown as FIGURE 16, wherein magnetic amplifiers are used to control the action of two 2-phase control motors. Here the difference in DC levels at XX^1 and YY^1 appears as a current differential in the magnetic

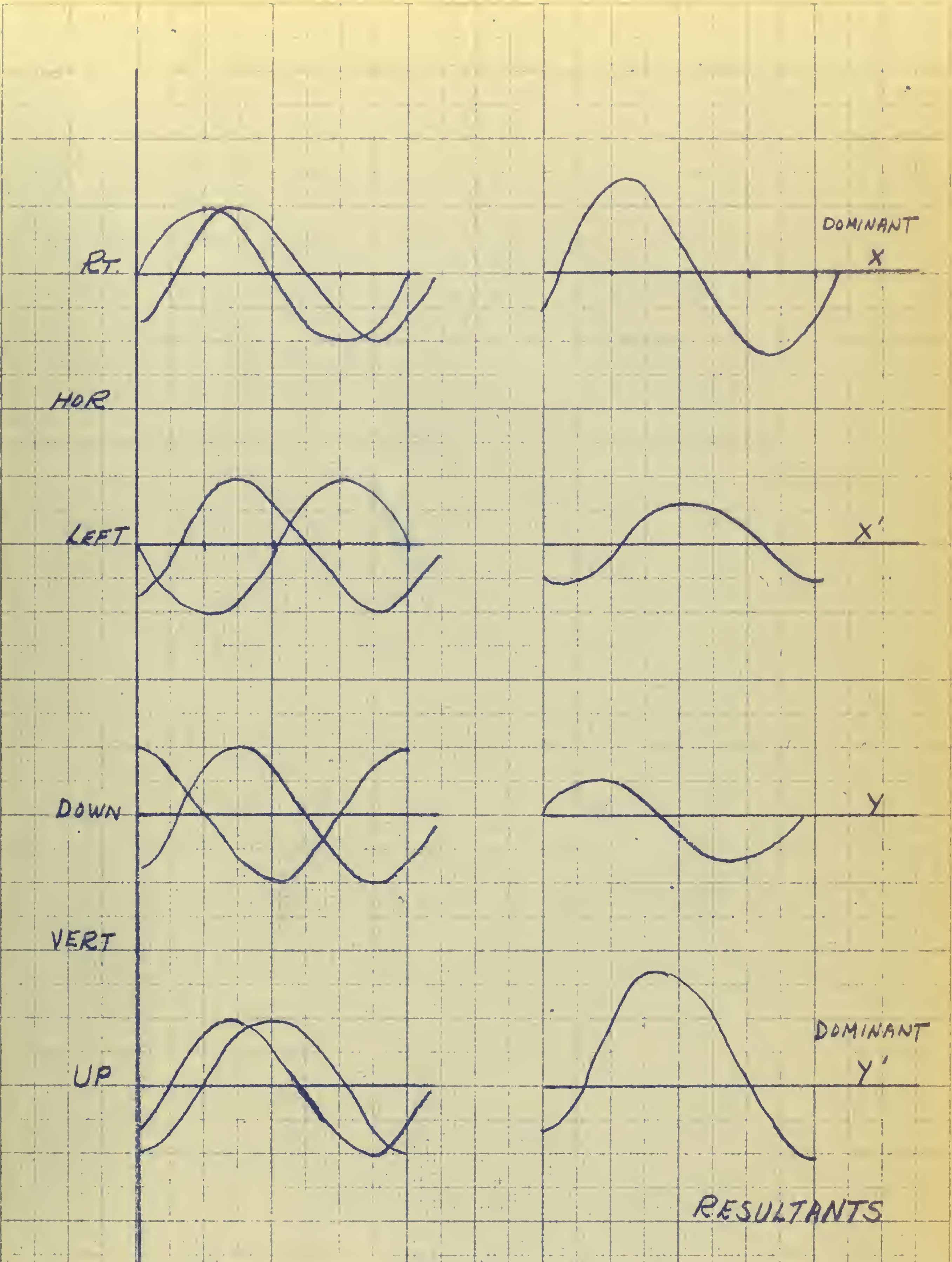

FIG. 15a POSITION 1

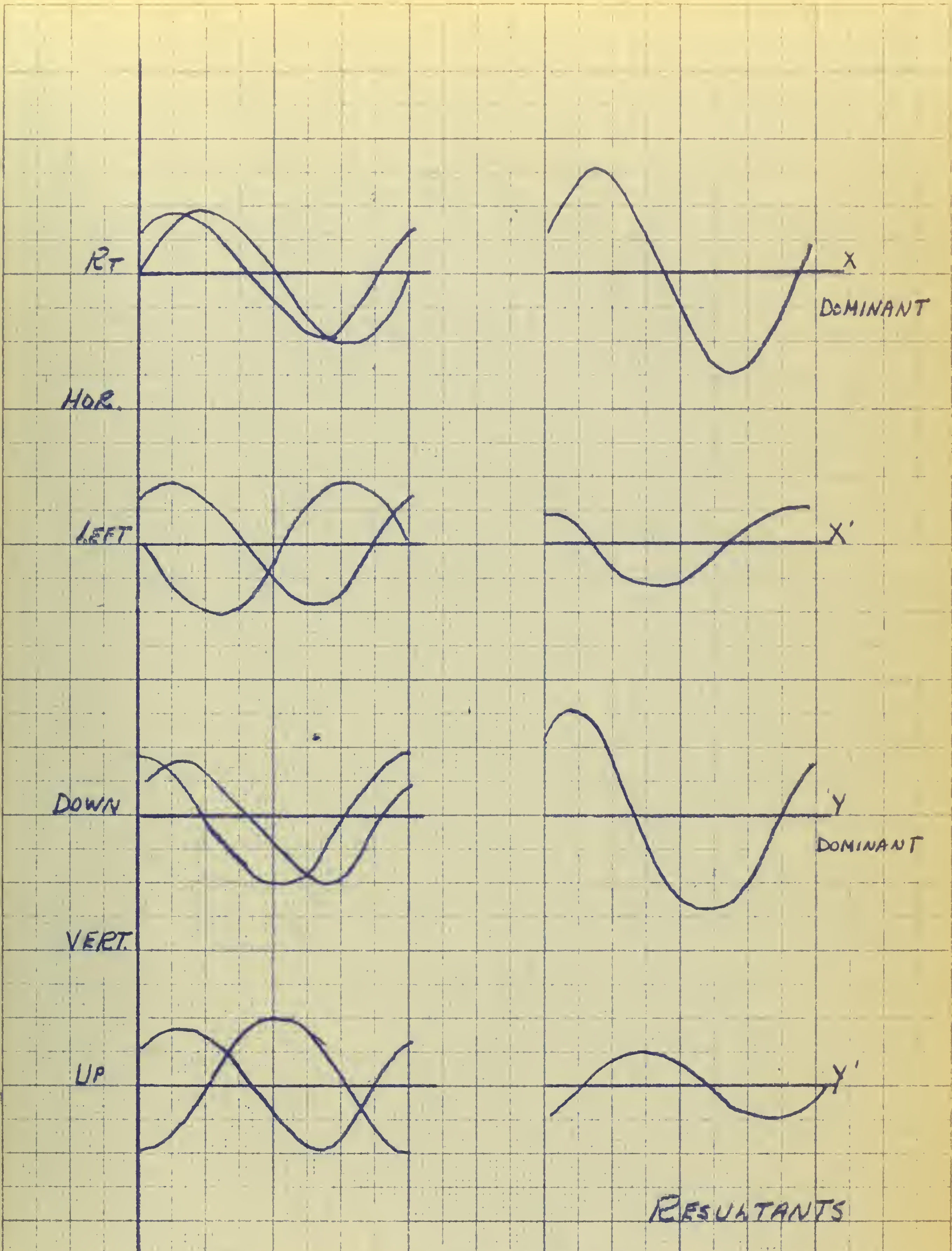
RT
HOR.
LEFT
DOWN
VERT.
UP
X
DOMINANT
X'
Y
DOMINANT
Y'
RESULTANTS

FIG 15b POSITION 2

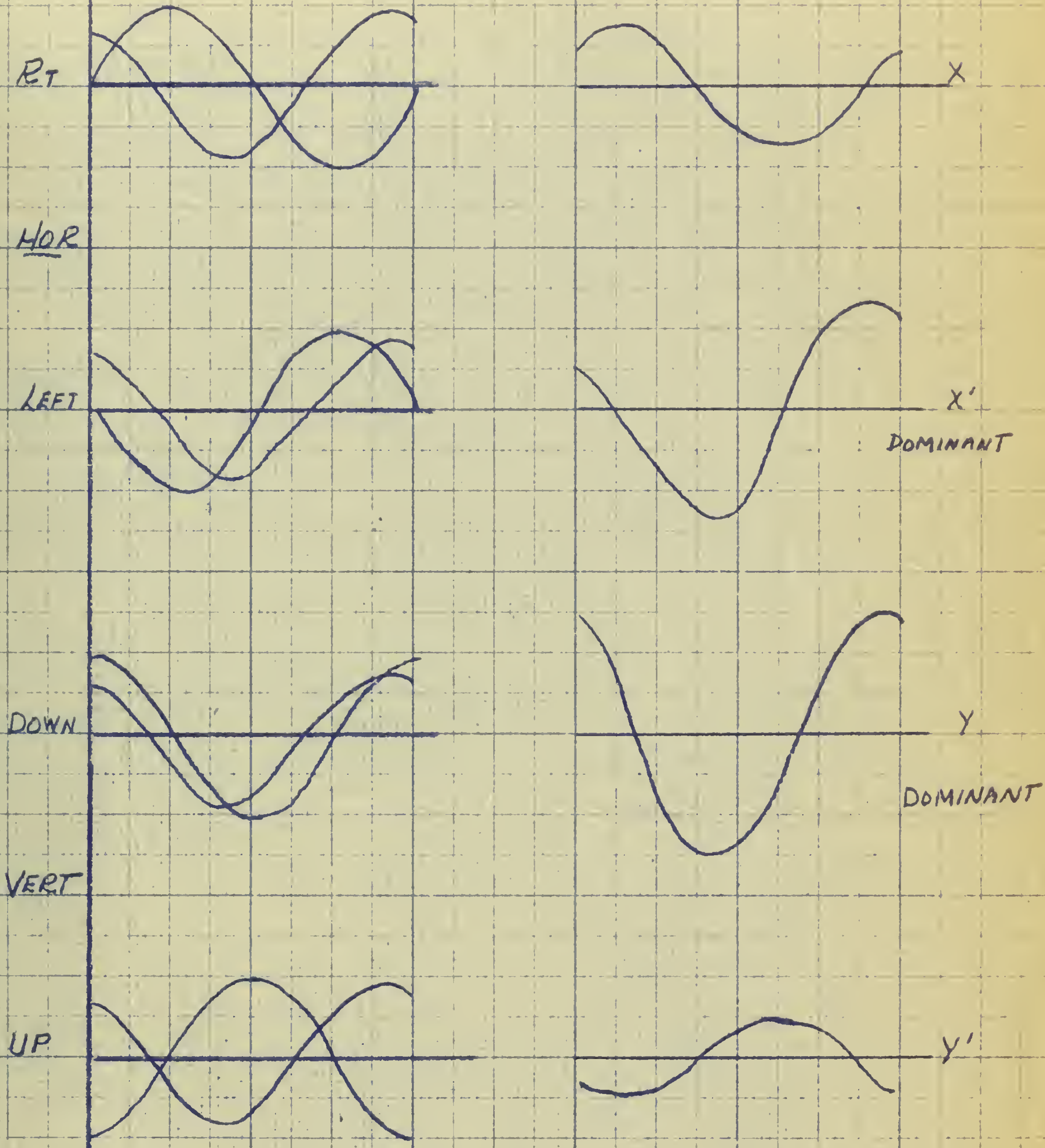

FIG. 15c POSITION 3 RESULTANTS

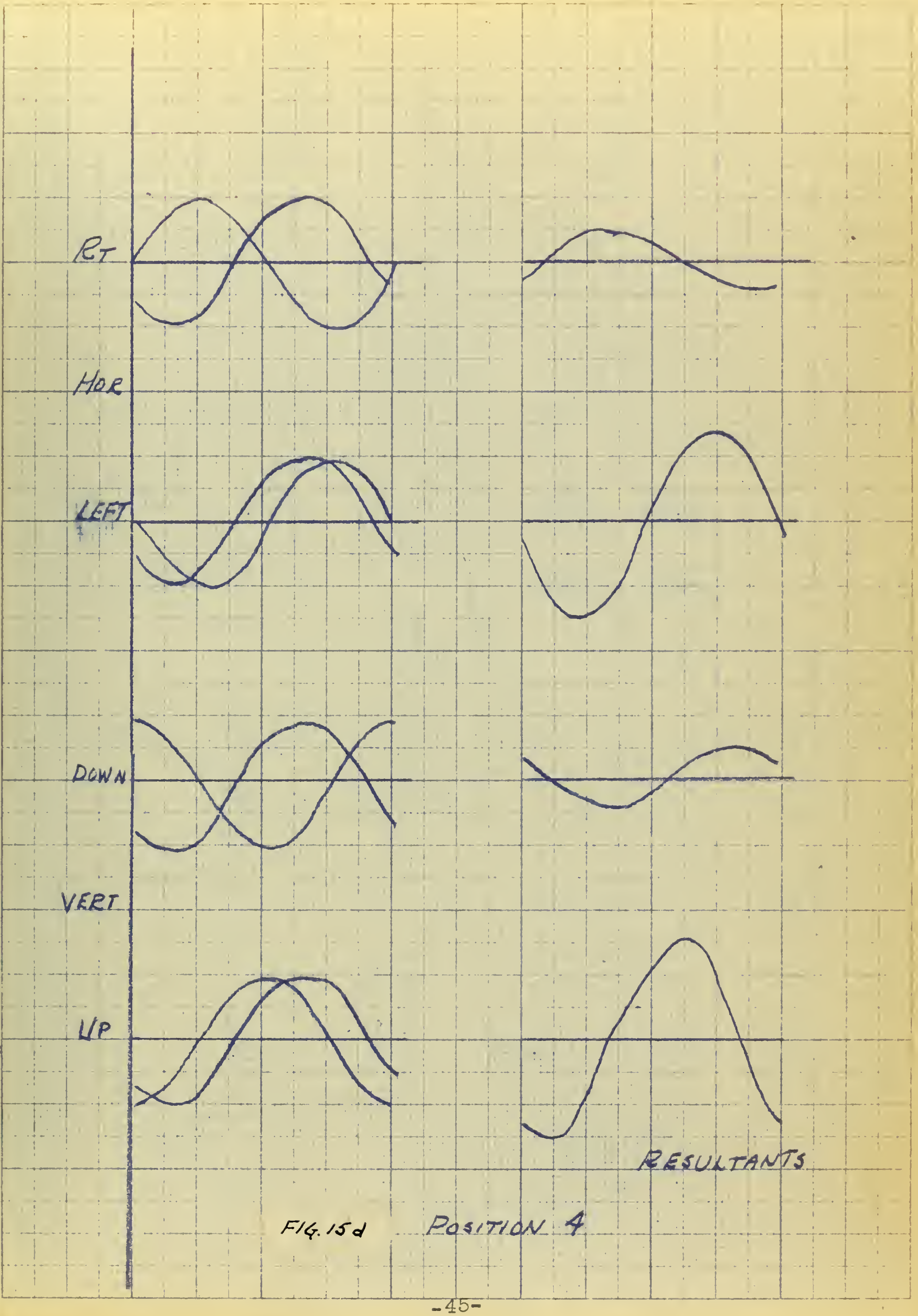

FIG. 15d   POSITION 4

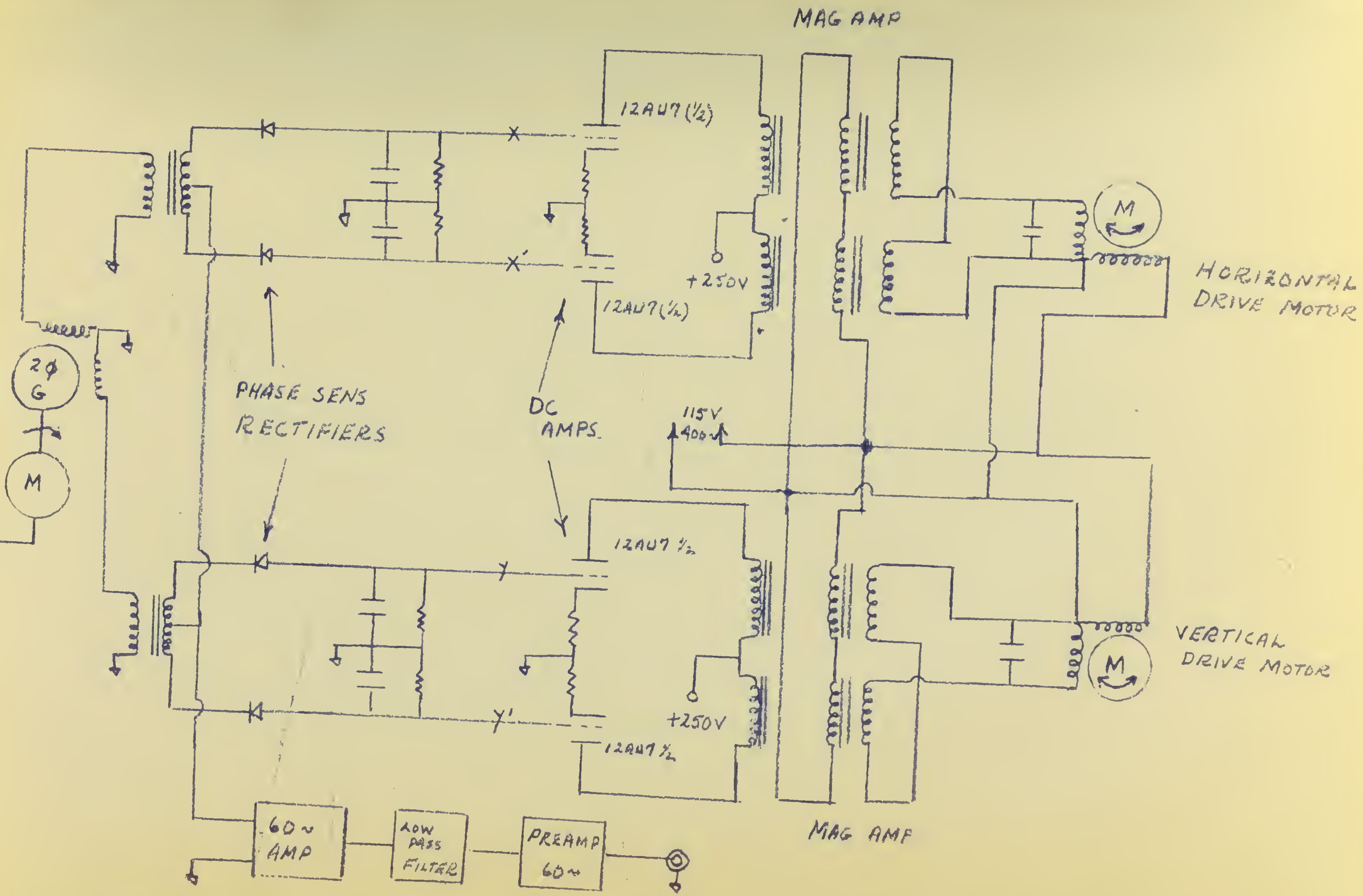
MAG AMP
12AU7 (½)
12AU7 (½)
+250V
HORIZONTAL DRIVE MOTOR
M
X
X'
PHASE SENS RECTIFIERS
DC AMPS.
115V 400~
2φ G
M
12AU7 ½
12AU7 ½
+250V
Y
Y'
VERTICAL DRIVE MOTOR
M
MAG AMP
60~ AMP
LOW PASS FILTER
PREAMP 60~

FIG. 16 Partial schematic showing error detection and servo drive circuits.

amplifier primary located in the push-pull DC amplifier plate circuits. The direction of flow in the control phase of the drive motors is then dependent on the dominant DC level at XX^1 and YY^1 respectively. The circuit is shown for a 400 cycle supply voltage, selected because the size of the resulting components is of the same order as the waveguide size.

At the position of match, the AC error signal has been shown in Chapter V and elsewhere to be a variation at twice the scanning frequency. Hence the inclusion of a low pass filter in the audio frequency amplifier so that this harmonic will not pass. This results in equal DC levels at points XX^1 and YY^1 (FIGURE 12), equal currents, in the DC amplifier plate circuits, and no current in the control phases of the drive motors. This marks the "null" position which will end the matching cycle.

The preceding discussion applies to the general case of initial mismatch wherein the magnitude of the two components of the modulation envelope are assumed to be of the same order of magnitude. It has been shown in Chapter V however, that the relative size may vary such that one is at a maximum while the other is a minimum. The greatest effect of an appreciable difference in magnitude between the components of the modulation envelope lies in the resultant value of the angle θ (using the notation of Chapter V). θ represents the departure of the phase angle of the modulation envelope from the 45° advance with respect to the horizontal component. Thus a phase ambiguity exists, approaching -45° where one component is on the order of 10 times the other. The

phase detection action under these conditions may be examined in a manner similar to that used for FIGURE 15. FIGURE 10 shows that in the region around station 5, the amplitude of the component of the modulation envelope due to the vertical sensing action is a minimum. The amplitude of the component due to horizontal sensing is a maximum at this station. Hence the modulation envelope will be of the form

$$E_r = R \sin \omega_s t$$

E_r = modulation envelope of reflected wave

R = magnitude of component of modulation envelope due to horizontal sensing motion

ω_s = angular frequency of rotation of the sensing probe

The subsequent phase detection action is shown in FIGURE 17. A "right" signal will be given to the horizontal drive motor, while the vertical drive motor receives no signal. The matching probe will soon be moved away from the narrow region of minimum vertical sense sensitivity.

The region of minimum horizontal sense sensitivity occurs near the positions of "most favorable" and "least favorable" match. This determines the required sensitivity of the audio frequency amplifier. Since the amplified error signal must be of the same order of magnitude as the reference phases, (about 12 volts peak*), the required amplification based on this minimum signal may be computed.

Assume that the minimum position error allowed corresponds to a VSWR of 1.05:1. This is based on the change in VSWR corresponding to the scanning radius of ".025 for the sensing probe as shown in

*Note: KEARFOTT SPIN GENERATOR XV - 1 - 16245

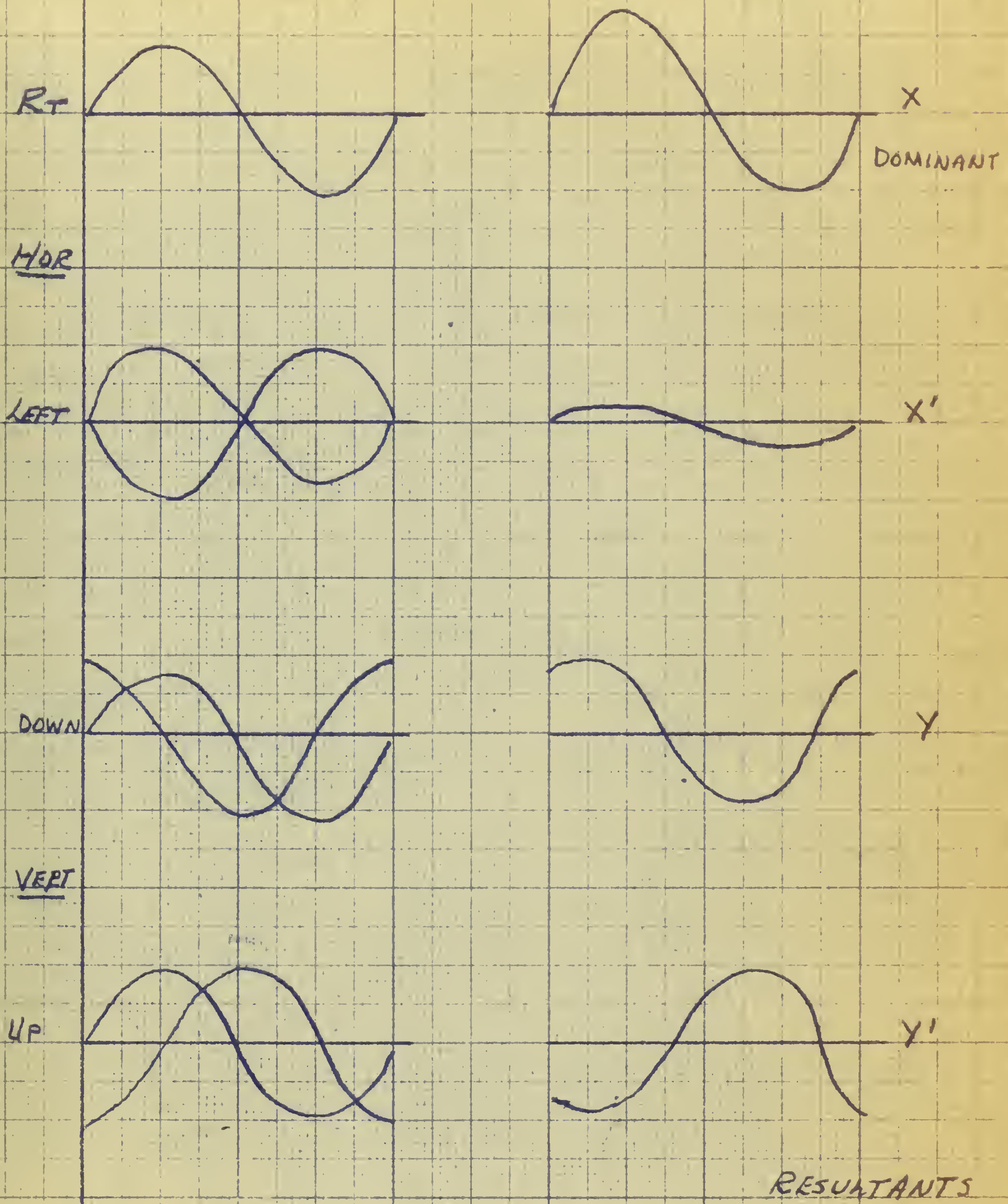

FIG. 17 PLOT OF $E_r = R \sin \omega_s t$ AS IT UNDERGOES PHASE DETECTION

FIGURE 6. Hence

For VSWR 1.05:1 = -32.3 db (level of reflected wave compared to incident wave)

Using 20 db directional coupler = -20.db (level of reflected wave in directional coupler compared to reflected wave in waveguide)

Total drop at detector = -52.3 db from incident wave.

Then, if 1 milliwatt incident in guide

$P_{detector} = 1.7 \times 10^{-3} \times 10^{-5} = 1.7 \times 10^{-8}$ watts

It is known that for typical crystal (1N23), the minimum detectable power is $.5 \times 10^{-8}$ watts which gives 1 μ volt across 200 ohms.*

If minimum incident wave considered is 20 milliwatts, commonly used in experimental work, then

$P_{detector} = 1.7 \times 10^{-8} \times 20 = 34 \times 10^{-8}$ watts

Since crystals are square law devices, **where doubling the power input doubles the voltage output, 34×10^{-8} watts gives 68 μ volts across 200 ohms. This represents the required sensitivity of the preamplifier. Total gain of audio frequency amplifier must then be in the neighborhood of 148,000.

In summary then, the servo amplifier and detector suggested in this chapter will function to position the probe assembly longitudinally and at the correct depth to affect a match for an unmatched load in a waveguide system.

---

*H.C. Torrey and C.A. Whitner, CRYSTAL RECTIFIERS, page 335 gives 1.5 μ amp/μ watt with no load resistance specified. The figure used above has been experimentally derived at Dalmo Victor Company, where this figure is specified as a basis for design.

**Ibid page 333 ff.

CHAPTER VII EXPERIMENTAL DATA

Experimental data was gathered in two phases: first, to investigate the modulation envelope variations due to each component of motion separately, and second, to investigate the variation of modulation envelope due to the circular scanning motion of the sensing probe. In each case a bench setup as shown in FIGURE 18 was used. The variation of the level of the reflected wave being the main point of interest, this was measured directly using a 10 db directional coupler* and an HP-415 power level meter.

Data in phase 1 was taken using the probe and carriage model as shown in FIGURE 19. This carriage allowed variations in the position of the sensing probe relative to the matching probe so that horizontal or vertical motion alone could be achieved. The data shown in FIGURE 20 is but one of many such sets taken and is shown as being typical of its kind, since there seems to be no logical way to combine the data for the many possible combinations of load, matching probe position and depth and frequency change into one diagram. Nor does there seem to be much to be gained from such a presentation. FIGURE 20 shows the variation due to horizontal displacements of sensing probe as shown for a longitudinal position which permitted a signal of sufficient strength to be read accurately on the test equipment available. The tunable klystron used (Varian X-13) suffers from power output variations of small magnitude but sufficient to make the acquisition of consistent data difficult, since the variation in the level of the reflected wave

---

*Note: This refers to the power level of the reflected wave in the directional coupler compared to that of the reflected wave in the waveguide.

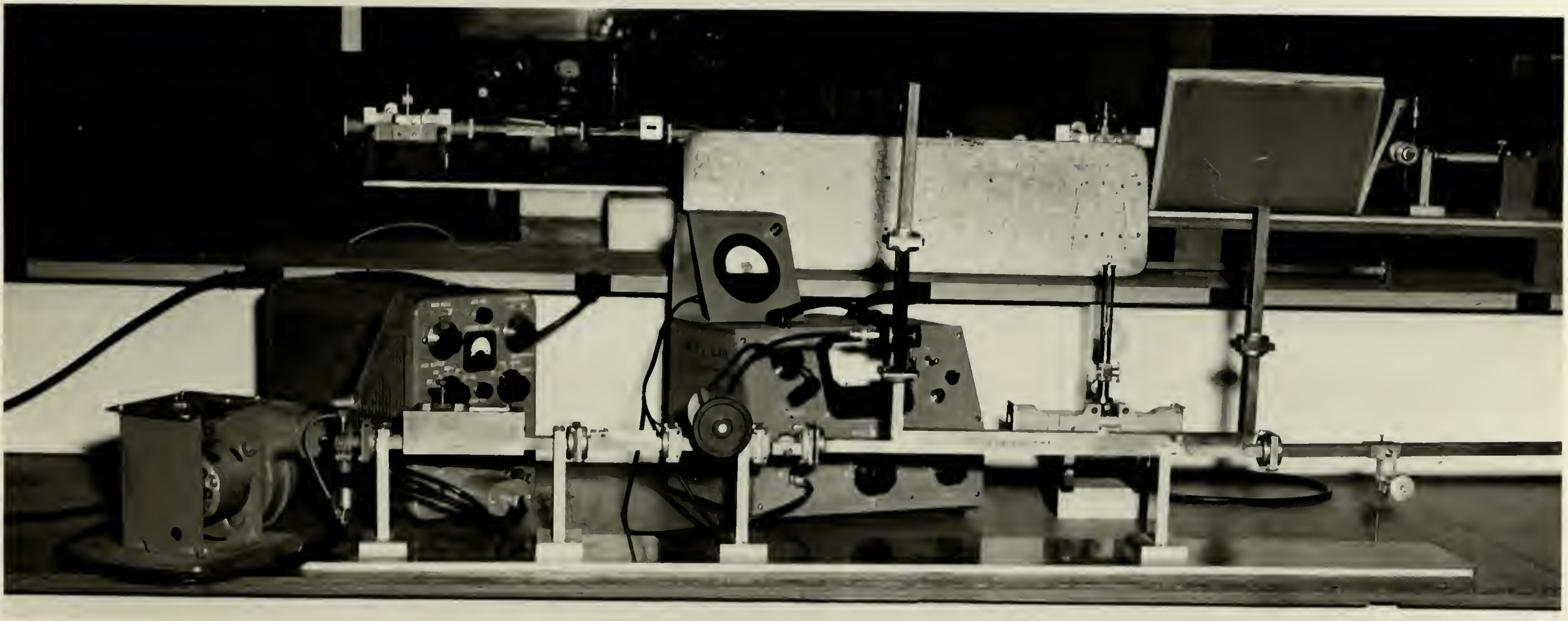

FIG. 15 Equipment used in acquiring data.

75682

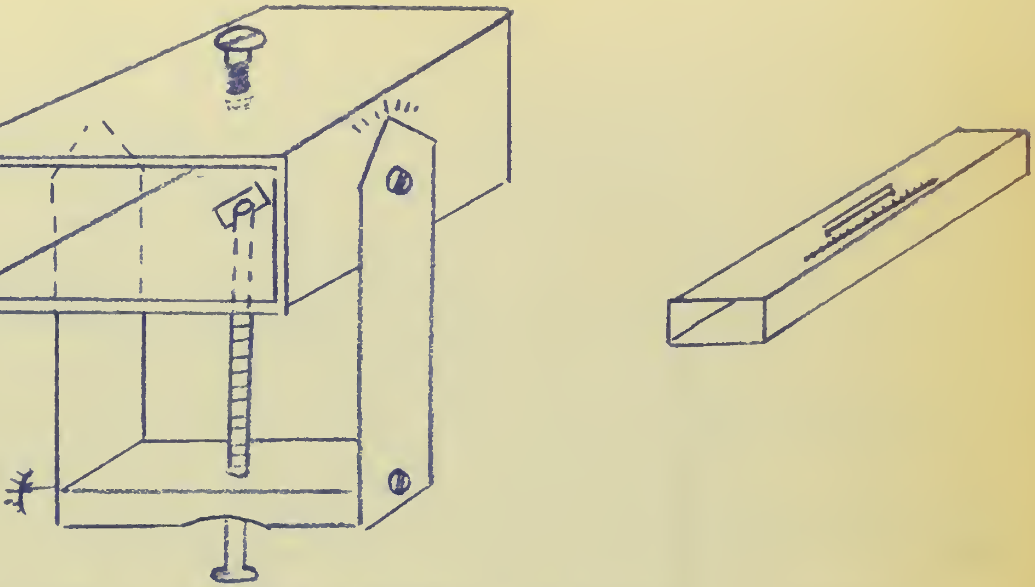

FIG. 19 Carriage as used to investigate variation of Er due to horizohtal and vertical components of motion.

FIG. 22 Carriage as used to investigate variation of Er due to circular scanning motion of sensing probe.

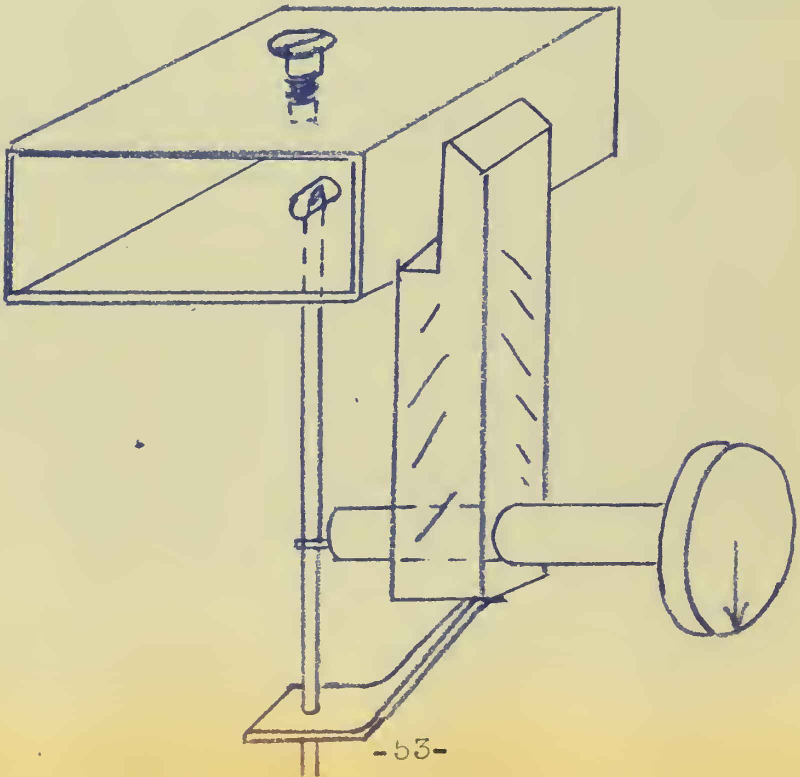

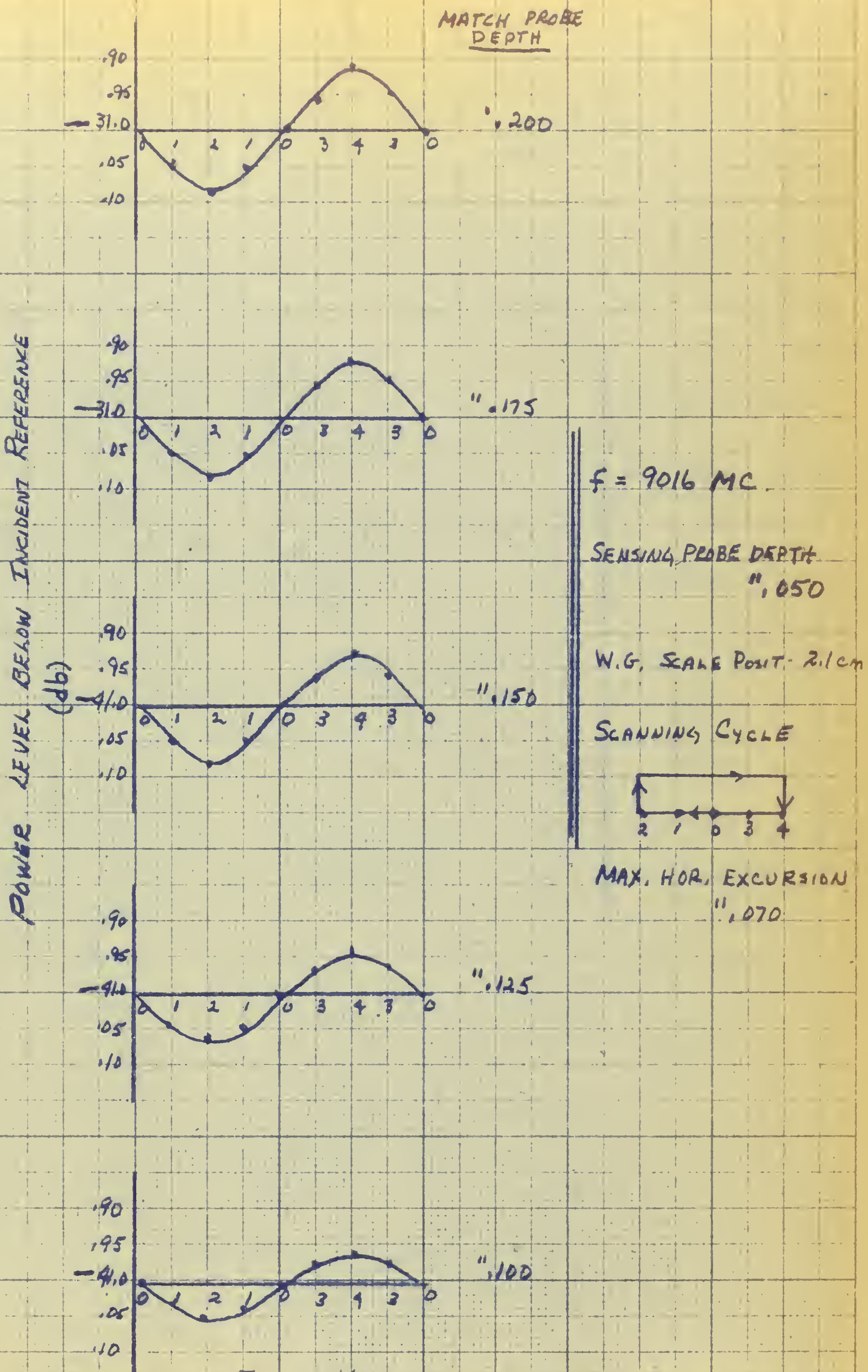

FIG. 20 VARIATION OF E_A IN db DUE TO HORIZONTAL MOTION OF SENSING PROBE AS SHOWN.

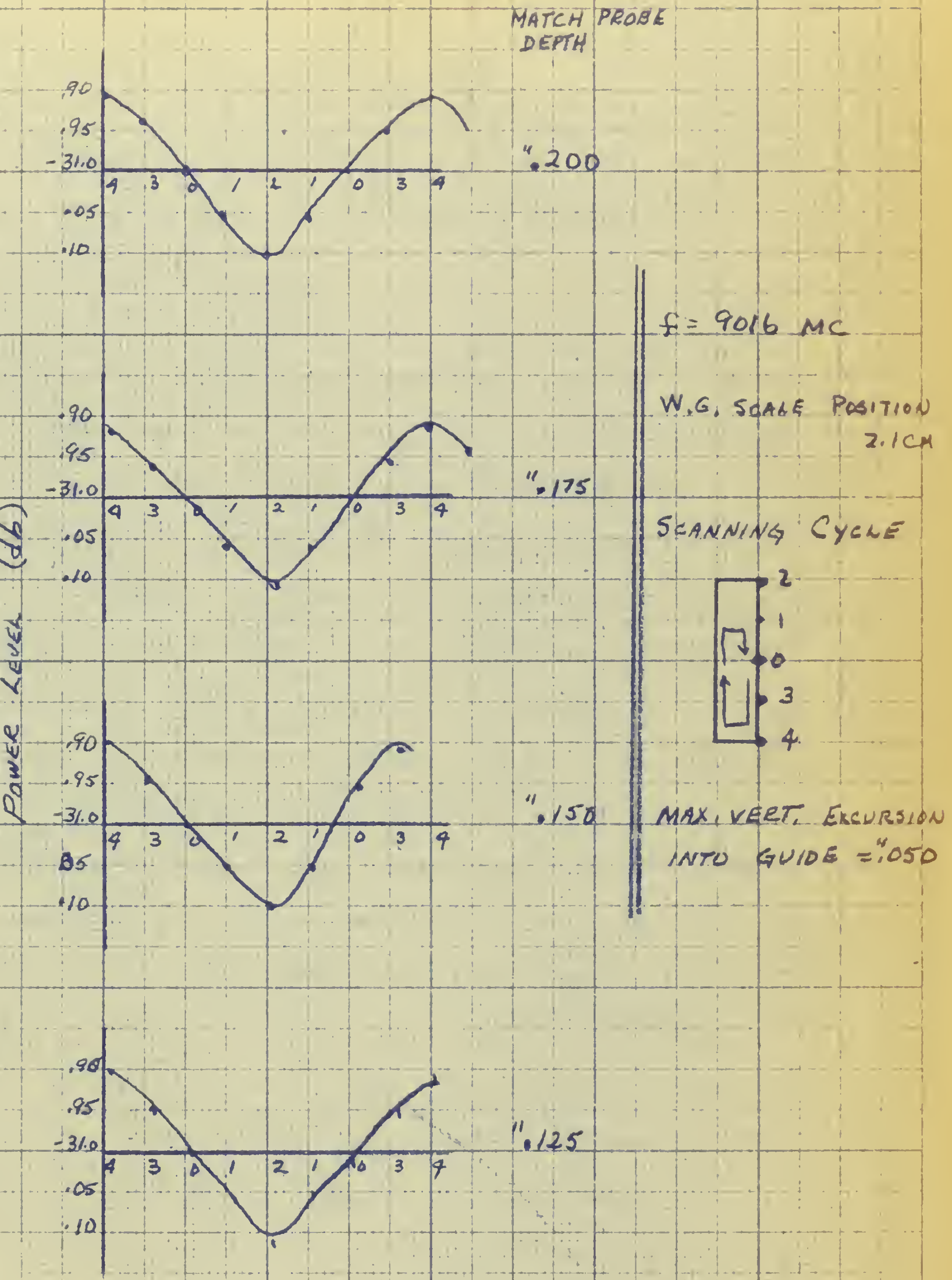

f = 9016 MC

W.G. SCALE POSITION 2.1CM

MAX. VERT. EXCURSION INTO GUIDE = ".050

FIG. 21 VARIATION OF E_r (db) DUE TO VERTICAL MOTION OF SCANNING PROBE AS SHOWN.

sought were small. Hence many runs were made, and FIGURE 20 represents an average of these runs.

FIGURE 21 shown the variation of the modulation envelope due to vertical displacements as indicated in the figure. The same comments given just above apply here also. The two sets of data shown do illustrate several points:

1. The waveforms of the modulation envelope due to the motion of the sensing probe along the paths previously described as the paths of the component harmonic motions which make up the circular scan (Chapter IV) are the sine and cosine waves predicted from the theoretical analysis. Furthermore, these separate waves are in phase with the position of the sensing probe relative to the reference position.

2. The order of magnitude of variation in power level of the reflected wave due to similar excursions of the sensing probe in either direction (i.e. horizontal and vertical) are about the same, so that other conditions being equal, the magnitude of the components due to each harmonic motion of the scan are equal.

The data for variation of the modulation envelope due to circular scanning motion of a sensing probe was taken using an assembly as shown in FIGURE 22. Here again the curves shown are subject to errors previously described, but are considered to be typical. Chosen to be represented are waveforms corresponding generally to those positions of the matching probe shown in FIGURE 11. These positions were found by a trial and error process, which process can be more quickly carried out on a bench set-up than they can be calculated. The resulting modulation envelope waveforms in FIGURE 23 are seen to be very similar

to those shown in FIGURE 12, and indicates that the experimental behavior bears out the conclusions made in the theoretical analysis.

POSITION OF MATCH ".175 PENETRATION AT 3.2 CM (ON W.G. SCALE)
SCANNING RADIUS ".030 (REF. PT. FOR SENSING PROBE SCAN ADJUSTED SO THAT AT REST IT PROJECTS ".150 INTO GUIDE. THIS GIVES GREATER VARIATION DURING SCAN, BETTER READINGS.)

NOTE: FOR MEANING OF POSITION ASSIGNMENTS REFER FIGS. 7 AND 8.

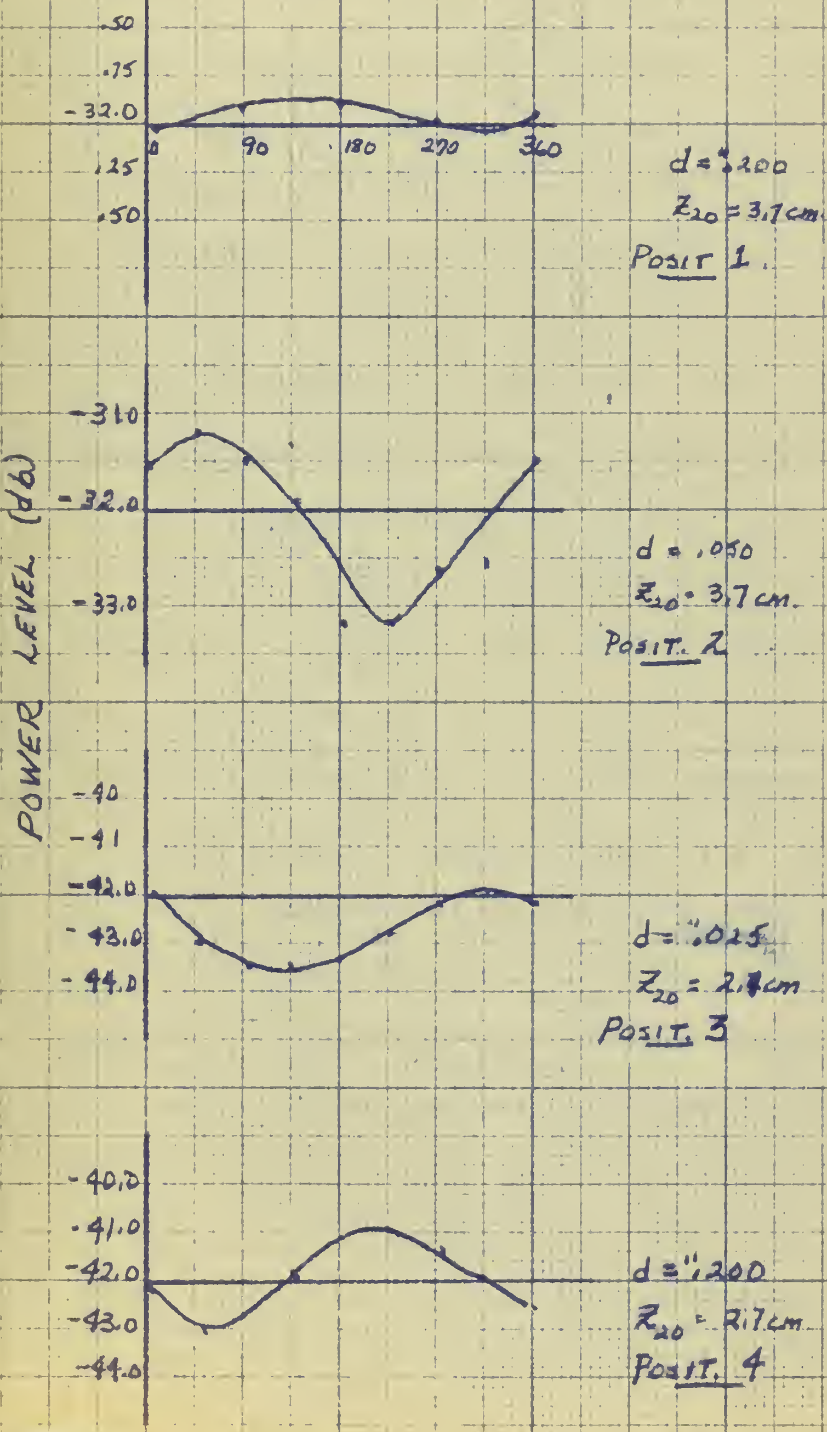

FIG. 23 WAVEFORMS OF E_R DUE TO SCANNING PROBE AT POSITIONS INDICATED

CHAPTER VIII CONCLUSION

It has been the purpose of this thesis to investigate and apply the susceptance probe for use in an automatic waveguide matching system. The servo loop design, and the manner of utilizing the AC component of the reflected wave are not to be taken as the final answer to the problem, but rather they are presented as a basis for further investigation. FIGURE 24 is a sketch of the proposed device as it is being constructed. The model, it has been found, cannot be made up satisfactorily except by skilled commercial facilities, since component dimensions and smooth mechancial operation are critical factors. When the model is available, further investigation will be required to definitely fix the manner of operation of the complete system.

It is felt however, on the basis of the investigation presented here, that the principles of operation are established: i.e., that a positioning signal can be derived from a mechanical circular scan of the sensing probe, the signal being made up of amplitude variations of the reflected wave, over a broad radio frequency range.

Other areas for investigation, once the operation of the device is attained, concern the adaptability of the automatic tuner to a high power microwave system, to an automatic phase plotting device, and refinements of the servo loop such that the tuner may follow cyclic variations of mismatch as are experienced with rotating joints and scanning dishes. The last named use refers to cyclic variations of a fairly low frequency. It is not likely that servo system design will permit the response times that would be required to follow the high speed conical scanning rates of some of the present day radar equipment.

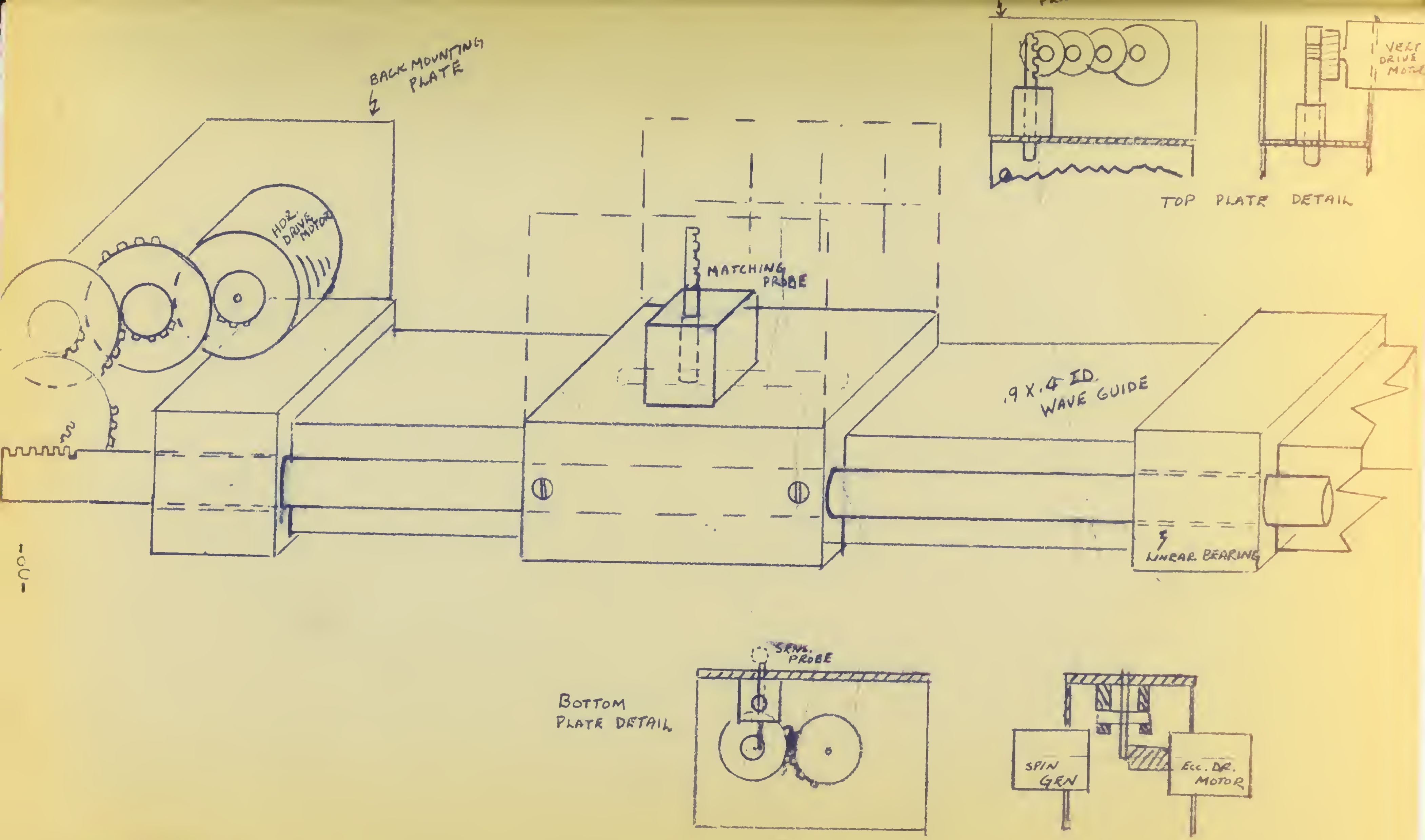
BACK MOUNTING PLATE
HOR. DRIVE MOTOR
MATCHING PROBE
.9 X .4 I.D. WAVE GUIDE
LINEAR BEARING
TOP PLATE DETAIL
VERT DRIVE MOT
BOTTOM PLATE DETAIL
SRNS. PROBE
SPIN GEN
ECC. DR. MOTOR

FIG. 24 Proposed mechanical layout for automatic waveguide tuning device.

BIBLIOGRAPHY

1. Ragan, G. L. - "Microwave Transmission Circuits"
MIT Radiation Laboratory Series, Vol. 9,
New York, McGraw Hill Book Company, 1948

2. Marcuvitz, N. - "Waveguide Handbook"
MIT Radiation Laboratory Series, Vol. 10,
New York, McGraw Hill Book Company, 1951

3. Southworth, G. C. - "Principles and Applications of Wave
Guide Transmission"
New York, Van Nostrand, 1950

4. Moreno, T. - "Microwave Transmission Design Data"
New York, McGraw Hill Book Company, 1948

5. Jakes, W. C., Jr. - "Broadband Matching With a Directional
Coupler"
Proceedings of the I.R.E., October 1952,
Page 1216

6. Brown, L.W. - "Problems and Practice in the Production
of Wave Guide Transmission Systems"
Journal of the Institute of Electrical
Engineers, Volume 93, Part III A, No. 4,
Page 639, London, 1946

7. Torrey, H.C. and Whitmer, C. A. -"Crystal Rectifiers"
MIT Radiation Laboratory Series, Volume 15,
New York, McGraw Hill Book Company, 1948

MR 14 63
20 JUL 68
18 FEB 69
[illegible]
4 MAY 71

1 1 4 0 9
1 6 5 4 7
1 7 3 4 1
[illegible]
1 8 6 0 0

Thesis 20609
R265 Red
Investigation of the
susceptance probe for
use in an automatio
waveguide matching
system

MR 14 63
20 JUL 68
18 FEB 69
[illegible]
4 MAY 71

1 1 4 0 9
1 6 5 4 7
1 7 3 4 1
[illegible]
1 8 6 0 0

Thesis 20609
R265 Red
Investigation of the susceptance
probe for use in an automatic
waveguide matching system.

Library
U. S. Naval Postgraduate School
Monterey, California

ARTISAN
GOLD LETTERING
AND
SMITH BINDERY
OAKLAND, CALIF.

thesR265
Investigation of the susceptance probe f
3 2768 002 05002 3
DUDLEY KNOX LIBRARY